ARMY RESEARCH LABORATORY

Frequency Doubler (from 4.7 to 9.4 GHz) Using a Diode

Jeffrey Himmel

ARL-TR-72

July 1994

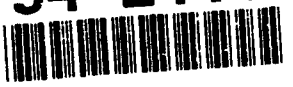

NOTICES

Disclaimers

The findings in this report are not to be construed as an official Department of the Army position, unless so designated by other authorized documents.

The citation of trade names and names of manufacturers in this report is not to be construed as official Government endorsement or approval of commercial products or services referenced herein.

REPORT DOCUMENTATION PAGE

Form Approved
OMB No. 0704-0188

1. AGENCY USE ONLY (Leave blank)	2. REPORT DATE	3. REPORT TYPE AND DATES COVERED
	July 1994	Technical Report: Feb 92 to May 93

4. TITLE AND SUBTITLE
FREQUENCY DOUBLER (FROM 4.7 TO 9.4 GHz) USING A DIODE

5. FUNDING NUMBERS
PE: 612705
PR: 1L162705 AH94
TA: CM
WU: 52MM02A

6. AUTHOR(S)
Jeffrey Himmel

7. PERFORMING ORGANIZATION NAME(S) AND ADDRESS(ES)
US Army Research Laboratory (ARL)
Electronics and Power Sources Directorate (EPSD)
ATTN: AMSRL-EP-MD
Fort Monmouth, NJ 07703-5601

8. PERFORMING ORGANIZATION REPORT NUMBER
ARL-TR-72

9. SPONSORING/MONITORING AGENCY NAME(S) AND ADDRESS(ES)

10. SPONSORING/MONITORING AGENCY REPORT NUMBER

11. SUPPLEMENTARY NOTES

12a. DISTRIBUTION/AVAILABILITY STATEMENT
Approved for public release; distribution is unlimited.

12b. DISTRIBUTION CODE

13. ABSTRACT (Maximum 200 words)

This report discusses the design, fabrication and testing of a harmonic generator which has an input frequency of 4.7 GHz and an output frequency of 9.4 GHz. A diode was used as the nonlinear device to produce the harmonics. The designed bandwidth of the output signal was 10 percent of the output frequency, with power optimized at 9.4 GHz.

14. SUBJECT TERMS
Frequency doubler; filter design

15. NUMBER OF PAGES
86

16. PRICE CODE

17. SECURITY CLASSIFICATION OF REPORT	18. SECURITY CLASSIFICATION OF THIS PAGE	19. SECURITY CLASSIFICATION OF ABSTRACT	20. LIMITATION OF ABSTRACT
Unclassified	Unclassified	Unclassified	UL

Contents

Figures

Tables

List of symbols

Symbol	Description	Units (Abbreviation)
B_k	Susceptance of the kth section	Mhos
BW	Bandwidth	Gigahertz (GHz)
E_{ff}	Efficiency of diode	-
f_a, f_b	Stopband-edges for bandpass filter	Gigahertz (GHz)
f_r	Resonant frequency of bandpass filter	Gigahertz (GHz)
freq	Design frequency (in "Microstrip" program)	Gigahertz (GHz)
f_s	Stopband-edge for lowpass prototype filter	Gigahertz (GHz)
f_1, f_2	Passband edges	Gigahertz (GHz)
g_k	immittance element value, i.e., normalized impedance or admittance	-
h	dielectric thickness (in "Microstrip" program)	Microns (μm)
h_2	height of metal casing above circuit ground plane	Microns (μm)

Symbol	Description	Units (Abbreviation)
L_m	Ripple factor of a filter	Decibels (dB)
L_s	Minimum insertion loss of stopband-edge	Decibels (dB)
l_s	Stub length	Centimeters (cm)
n	Number of filter sections	-
R_b	Bias resistance	Ohms (Ω)
$S_{pk,k+1}$	Spacing between the resonators of resonator pair #k,k+1	Microns (μm)
t	copper thickness	Microns (μm)
W	Width of transmission line section (in "Microstrip" program)	Microns (μm)
Y_k	Characteristic admittance of the kth section of transmission line	Mhos
Z_k	Characteristic impedance of the kth section of transmission line	Ohms (Ω)
Z_0	Characteristic impedance of transmission line	Ohms (Ω)

Symbol	Description	Units (Abbreviation)
ε_r	Dielectric constant, or relative permittivity	-
λ	Wavelength in a transmission line	Meter (m)
ω_s'	Stopband-edge, $2\pi f_s$	Radians/second
ω_1'	Passband edge, $2\pi f_1$	Radians/second

Principles of Frequency Doubling with a Diode

The generation of harmonics with a diode can be conceptualized from the viewpoint of the current-voltage (I-V) curve of the general diode, as illustrated in **Figure 1.** Due to the nonlinearity of the diode, a sinusoidal signal that passes through the diode gets distorted. The distorted output signal, by definition, must have higher frequency Fourier components.

The basic schematic of the frequency doubler is illustrated in **Figure 2.** The doubler was matched to 50 ohm lines. The lowpass filter serves the purpose of preventing reflections of the higher harmonics from reaching the frequency source. This allows the source to produce a clean signal. It also helps prevent noise from the frequency source at the desired doubled frequency from reaching the diode and the output port of the doubler. The bandpass filter allows only the desired harmonics to reach the output port. The resistor R_b determines the dc bias of the diode.

The manufacturer which supplied the diode for this project was M/A-COM, Inc. The diode which M/A-COM recommended is a "dual-mode" diode, part #MA44706. The term "dual mode" is jargon used by M/A-COM to refer to the two specific mechanisms in this type of diode which produce the harmonics. One mechanism is the abrupt change in diode capacitance versus bias voltage, as illustrated in **Figure 3.** [1]

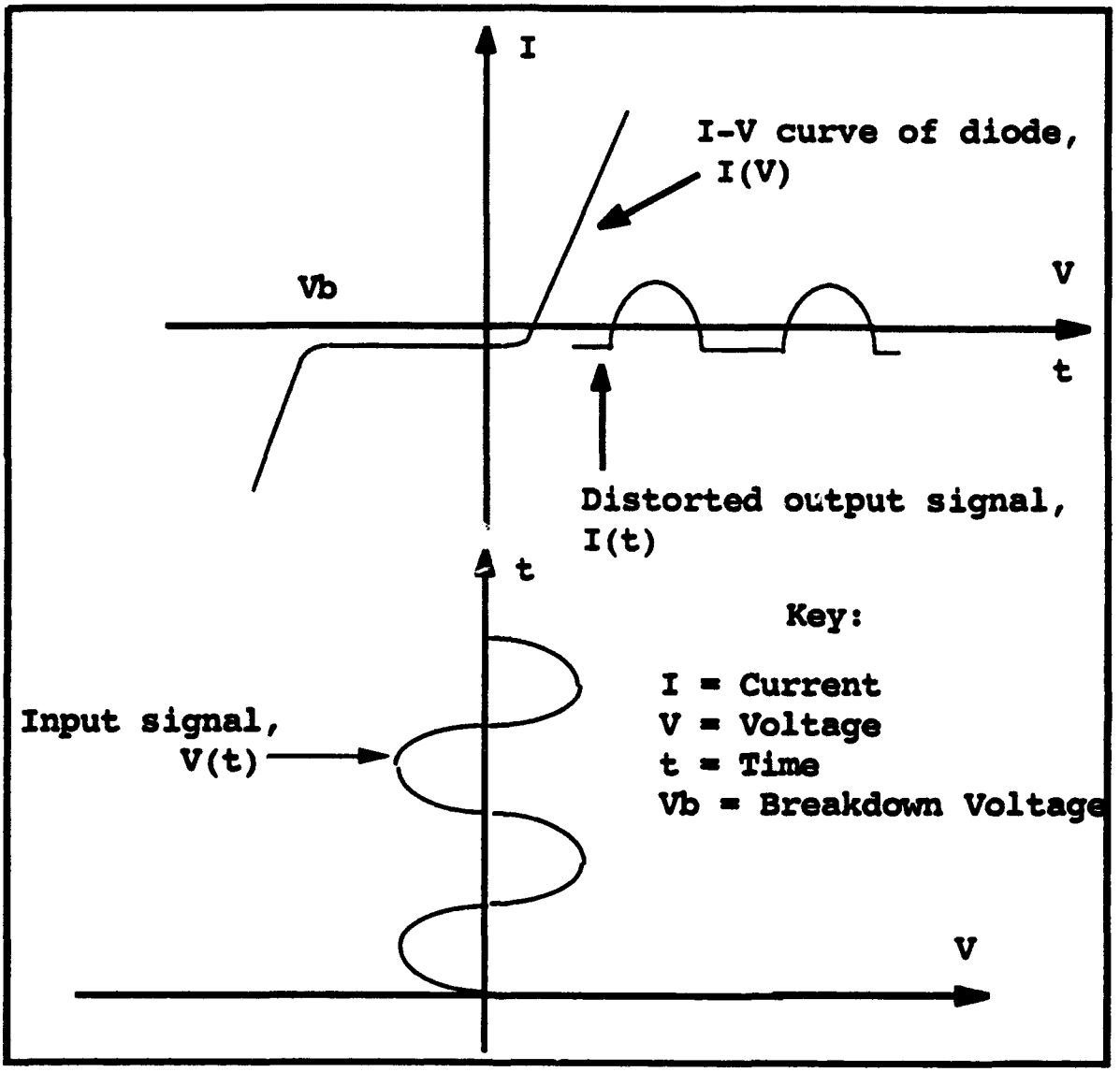

Figure 1: Representation of signal distortion by the diode.

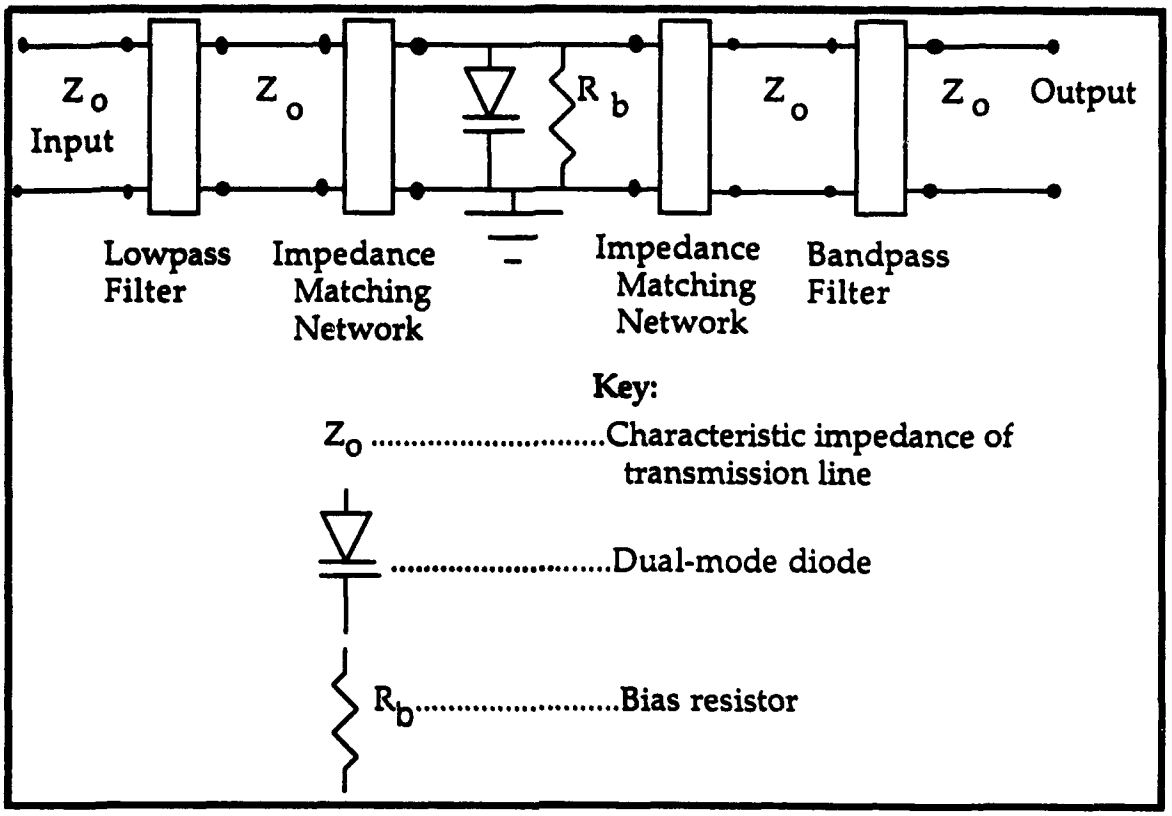

Figure 2: Basic schematic of frequency doubler

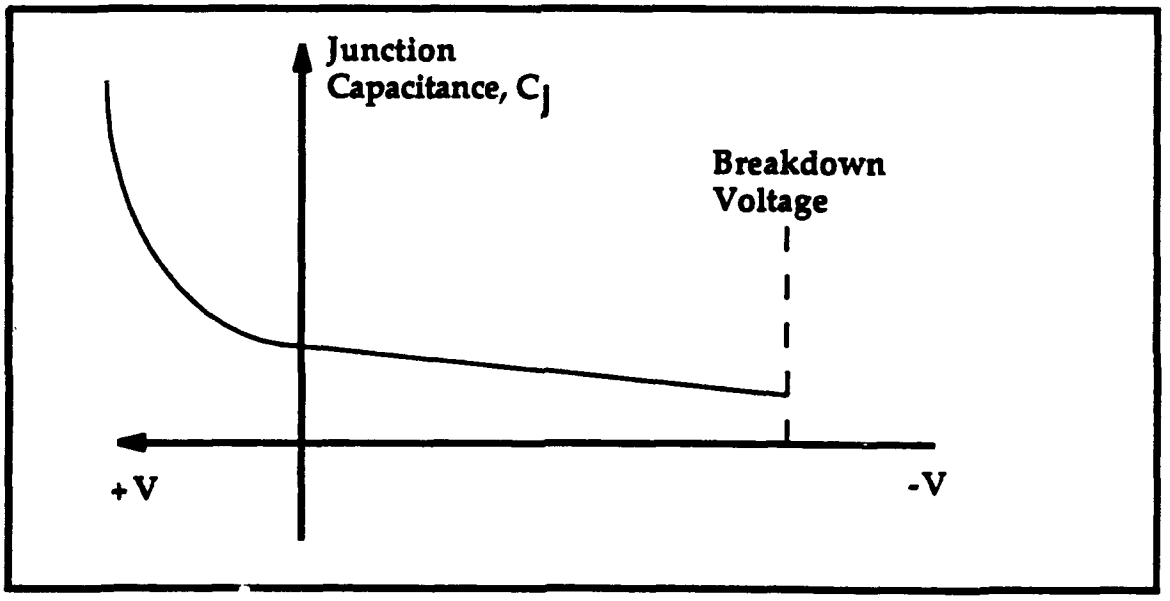

Figure 3: Dual-mode diode capacitance voltage law.

The other harmonics-producing mechanism in a dual mode diode is an abrupt change in charge versus input drive voltage. During the positive half of a sinusoidal signal, charge is stored. This charge is then extracted during the negative half of the cycle. The diode has a low impedance until it is completely discharged. The charge is completely extracted before the end of the negative half of the cycle, at which time the diode stops conducting, creating a sudden change (snap) to high impedance, as illustrated in **Figure 4.** [2] The time period from the start of the cycle, when the diode begins to charge up, to the end of discharge is called the **lifetime.** [3] The snap causes the formation of a voltage pulse, which may be rich in harmonics. **Snaptime** is the time it takes for the diode to change from conducting to nonconducting during the snap. [4]

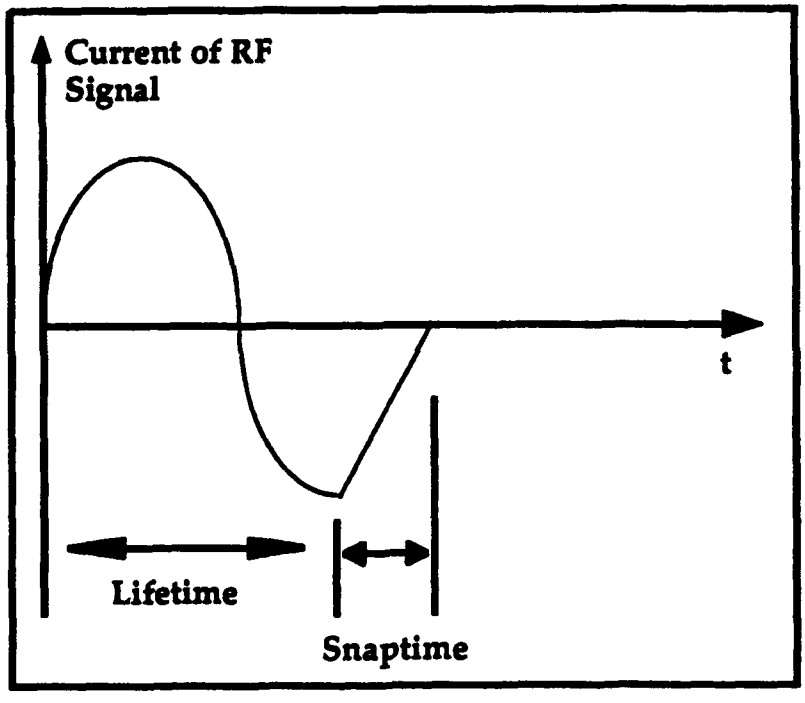

Figure 4: Snap of a dual-mode diode.

The efficiency of the diode E_{ff} may be affected by the diode's upper cutoff frequency, as expressed by the following equation:

$$E_{ff} = \exp(-\alpha F_{out}/F_c) \qquad (1)$$

where α is a constant which depends on the drive level and the capacitance voltage law of the diode, F_{out} is the desired output frequency in GHz, and F_c is the cutoff frequency of the diode in GHz at a self bias voltage (usually about -6 volts). For a dual mode diode at a drive level of -6 volts, $\alpha = 6.9$. [5]

Taking the natural log of both sides of equation (1) and solving for F_c, the following equation is obtained:

$$F_c = -\alpha F_{out}/\ln(E_{ff}). \qquad (2)$$

Multiplier diodes used in x2 multiplication tend to have efficiencies up to 60%. [6] Using equation (2), and plugging in several values of efficiency, values of cutoff frequency have been calculated and tabulated in **Table 1**.

Table 1: Diode efficiency vs. diode cutoff frequency

Diode Efficiency	Diode Cutoff Frequency, GHz
60%	127
20%	40
10%	28
1%	14

From **Table 1**, it becomes obvious that the theoretical values of cutoff frequency are likely to be comfortably higher than the desired output frequency of 9.4 GHz. Most modern dual-

mode diodes have cutoff frequencies of 200 to 300 GHz minimum. [7] The MA44706 diode is listed in the M/A-COM Semiconductor Products Master Catalog #SP101 as having a minimum cutoff frequency of 200 GHz, which is much higher than the theoretical values.

Figure 5 illustrates the diode model recommended by M/A-COM. The inductance L is assumed to be negligible. Junction resistance and capacitance vary nonlinearly with the signal voltage.

Most dual mode diodes work best with self bias, which is controlled by a bias resistor R_b in parallel with the diode. The power of the input signal sets up a dc bias level, so that R_b controls the current through the diode. [8]

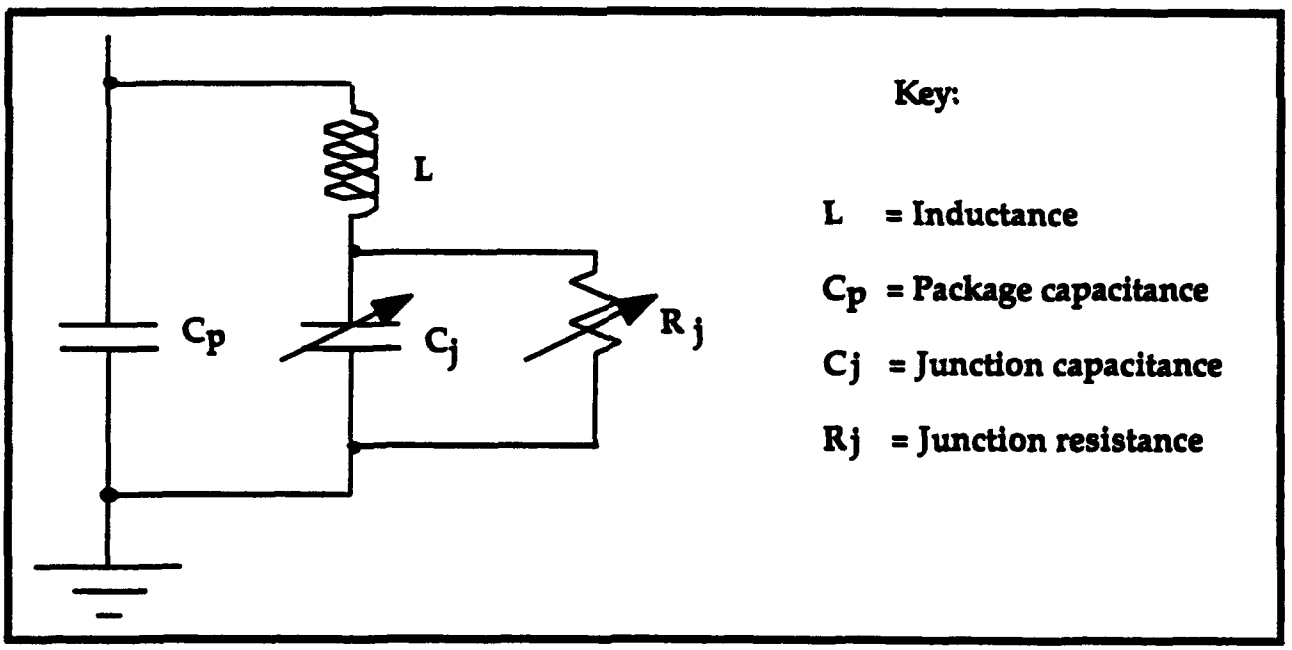

Figure 5: Model of dual mode diode as recommended by M/A-COM.

For dual-mode diodes, the suggested bias resistance is given by

$$R_b = \frac{10T_L}{(N^2)(C_{T-6})} \qquad (3)$$

where T_L is the lifetime in seconds, N is the multiplication order (2 in the case of a frequency doubler) and C_{T-6} is the total diode capacitance at -6 volts. [9]

Based on the diode model, assuming L is negligible, $C_{T-6} = C_j + C_p$, since the sum of parallel capacitances give the total capacitance. Thus, equation (3) becomes

$$R_b = \frac{10T_L}{(N^2)(C_j + C_p)} \; . \qquad (4)$$

The manufacturer indicated that the junction capacitance of dual mode diode #MA44706 tends to vary from diode to diode between 0.3 pF and 0.5 pF when a bias voltage of -6 volts is applied. [10]

Table 2, lists data on the #MA44706 diode necessary for calculating R_b.

Table 2: Manufacturer Data on the #MA44706 Diode [11]

Parameter	Value
Junction Capacitance, C_j	0.4 pF
Package Capacitance, C_p	0.18 pF
Lifetime, T_L	10 ns

Using the information in **Table 2**, the bias resistance R_b was calculated as follows:

$$R_b = \frac{10T_L}{(N^2)(C_j + C_p)}$$

$$= \frac{10(10 \times 10^{-9}\ s)}{(2)^2(0.4 \times 10^{-12}\ F + 0.3 \times 10^{-12}\ F)} = 35,714.3\ \Omega$$

The manufacturer suggested the use of a variable resistor since the actual value of R_b may vary substantially from the theoretical calculated value. The calculation above provides only a rough starting point.

Input Lowpass Filter Design

The lowpass filter was designed to allow frequencies up to 4.7 GHz to pass through it. However, in order that the frequency doubler be relatively wide band, it was necessary to allow frequencies a little higher through the filter. Therefore, an upper frequency passband-edge of about 6 GHz was chosen.

The design process of a microstrip filter, as outlined by Bahl [12], consists of three basic steps. The first step is to design a prototype lowpass filter with the desired passband characteristics. The second step consists of a transformation of the prototype network to the required type of filter (lowpass, highpass, bandpass or bandstop) with specified center and/or band-edge frequencies. The third step is the realization of the network in terms of lumped and/or distributed circuit elements. **Figure 6** illustrates the parameters of interest for the lowpass filter [13]. A Chebyshev filter model was assumed, with the passband-edge

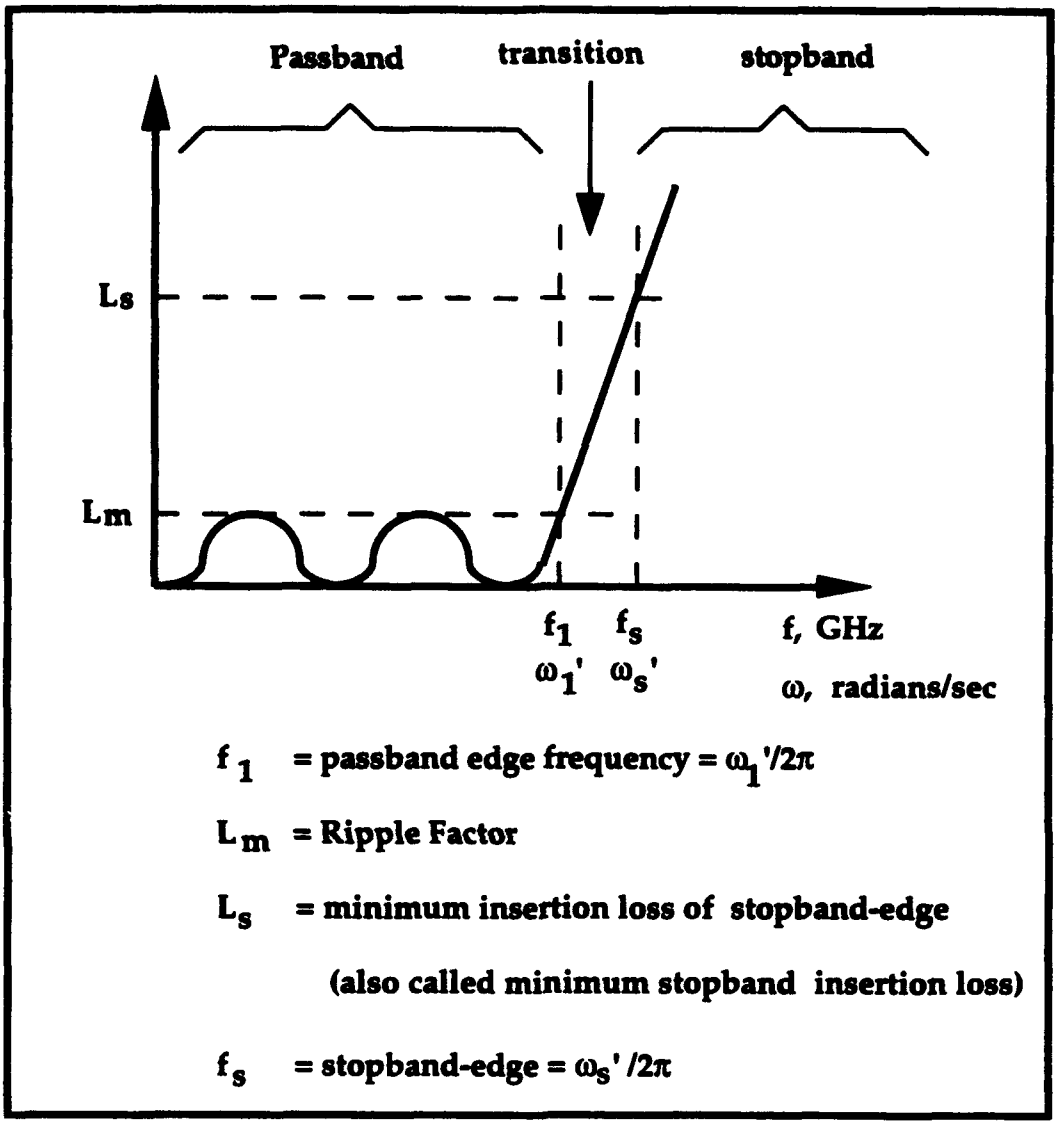

Figure 6: Parameters of interest for the lowpass filter.

frequency represented by f_1, the ripple factor represented by L_m, the stopband-edge represented by f_s, and the minimum stopband-edge insertion loss designated by L_s. Two notations for the frequency domain are shown in **Figure 6** since some authors prefer to represent the frequency in terms of GHz while others prefer to represent it in terms of radians per second. The cutoff frequency f_c is defined where the signal power is half the peak power in the passband. Usually, f_1 is only slightly less than f_c, so for all practical purposes f_1

and f_c are approximately equal.

In designing the lowpass filter, the author made some significant errors. The following discussion on the correct design is, in turn, followed by a discussion of the incorrect design and the results.

The correct design process was initiated by choosing f_1, f_s and L_s, and calculating f_s/f_1, or ω_s'/ω_1'. These parameters were applied to the nomograph illustrated in **Figure 7** in order to determine the number of sections n the filter should have [14]. In the nomograph, the scale labeled "Insertion Loss - dB" refers to L_s.

Table 3 illustrates two trials of parameters and the resulting number of sections. For Chebyshev filters, an even number of sections yields different values for the first normalized immittance element value g_0 and the last (load) element value g_{n+1}. This is undesirable since an impedance matching network would then be necessary to return to a 50 ohm line. Thus, an odd number of elements was favored.

Table 3: Two trials of lowpass filter design parameters and the resulting number of sections.

L_m	L_s	f_1	f_s	f_s/f_1	n	Comments
0.2	30	6.0	19.2	3.2	3	Preferred
0.2	30	6.0	13.2	2.2	4	Not desired

Figure 8 illustrates the lowpass prototype filter for n = 3. The series element values, g_1 and g_3, represent normalized impedances. The shunt element value g_2 represents a normalized admittance. The first element value g_0 represents

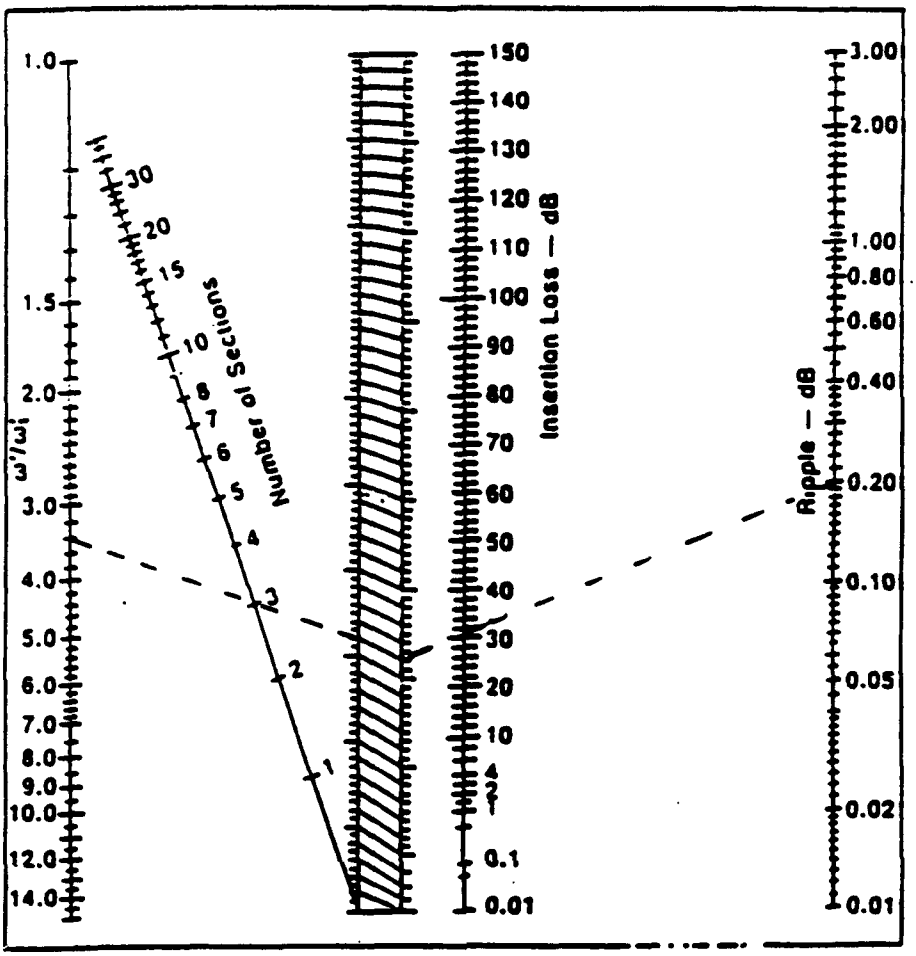

Figure 7: Nomograph for selecting number of sections of Chebyshev filter for given ripple and insertion loss in stopband.

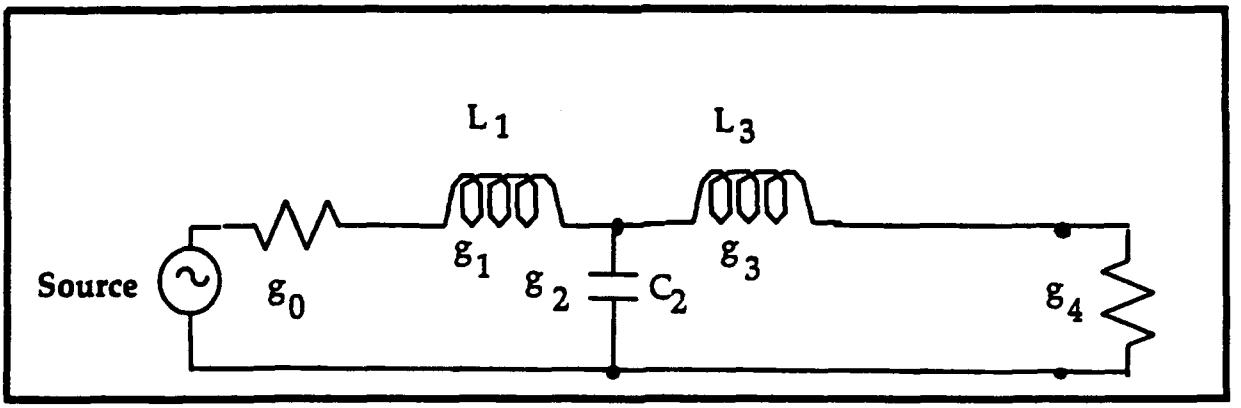

Figure 8: Circuit diagram of lowpass prototype filter (lumped-element model).

Table 4: Element values for a Chebyshev lowpass prototype filter. Note that $g_0 = 1$.

Value of n	g_1	g_2	g_3	g_4	g_5	g_6	g_7	g_8	g_9	g_{10}	g_{11}
					0.01-*dB Ripple*						
1	0.0960	1.0000									
2	0.4488	0.4077	1.1007								
3	0.6291	0.9702	0.6291	1.0000							
4	0.7128	1.2003	1.3212	0.6476	1.1007						
5	0.7563	1.3049	1.5773	1.3049	0.7563	1.0000					
6	0.7813	1.3600	1.6896	1.5350	1.4970	0.7098	1.1007				
7	0.7969	1.3924	1.7481	1.6331	1.7481	1.3924	0.7969	1.0000			
8	0.8072	1.4130	1.7824	1.6833	1.8529	1.8193	1.5554	0.7333	1.1007		
9	0.8144	1.4270	1.8043	1.7125	1.9057	1.7125	1.8043	1.4270	0.8144	1.0000	
10	0.8196	1.4369	1.8192	1.7311	1.9362	1.7390	1.9066	1.8527	1.5817	0.7446	1.1007
					0.1-*dB Ripple*						
1	0.3052	1.0000									
2	0.8430	0.6220	1.3554								
3	1.0315	1.1474	1.0315	1.0000							
4	1.1088	1.3061	1.7703	0.8180	1.3554						
5	1.1468	1.3712	1.9750	1.3712	1.1468	1.0000					
6	1.1681	1.4039	2.0562	1.5170	1.9029	0.8618	1.3554				
7	1.1811	1.4228	2.0966	1.5733	2.0966	1.4228	1.1811	1.0000			
8	1.1897	1.4346	2.1199	1.6010	2.1699	1.5640	1.9444	0.8778	1.3554		
9	1.1956	1.4425	2.1345	1.6167	2.2053	1.6167	2.1345	1.4425	1.1956	1.0000	
10	1.1999	1.4481	2.1444	1.6265	2.2253	1.6418	2.2046	1.5821	1.9628	0.8863	1.3554
					0.2-*dB Ripple*						
1	0.4342	1.0000									
2	1.0378	0.6745	1.5386								
3	1.2275	1.1525	1.2275	1.0000							
4	1.3028	1.2844	1.9761	0.8468	1.5386						
5	1.3394	1.3370	2.1660	1.3370	1.3394	1.0000					
6	1.3598	1.3632	2.2394	1.4555	2.0874	0.8636	1.5386				
7	1.3722	1.3781	2.2756	1.5001	2.2756	1.3781	1.3722	1.0000			
8	1.3804	1.3875	2.2963	1.5217	2.3413	1.4025	2.1349	0.8872	1.5386		
9	1.3860	1.3938	2.3093	1.5340	2.3728	1.5340	2.3093	1.3938	1.3860	1.0000	
10	1.3901	1.3983	2.3181	1.5417	2.3904	1.5536	2.3720	1.5066	2.1514	0.9034	1.5386
					0.5-*dB Ripple*						
1	0.6986	1.0000									
2	1.4029	0.7071	1.9841								
3	1.5963	1.0967	1.5963	1.0000							
4	1.6703	1.1926	2.3661	0.8419	1.9841						
5	1.7058	1.2296	2.5408	1.2296	1.7058	1.0000					
6	1.7254	1.2479	2.6064	1.3137	2.4758	0.8696	1.9841				
7	1.7372	1.2583	2.6381	1.3444	2.6381	1.2583	1.7372	1.0000			
8	1.7451	1.2647	2.6564	1.3590	2.6964	1.3389	2.5093	0.8796	1.9841		
9	1.7504	1.2690	2.6678	1.3673	2.7239	1.3673	2.6678	1.2690	1.7504	1.0000	
10	1.7543	1.2721	2.6754	1.3725	2.7392	1.3806	2.7231	1.3486	2.5239	0.8842	1.9841

normalized impedance as seen from the filter when looking towards the signal source. The last element value g_4 represents normalized impedance as seen by the filter towards the right, i.e., it represents the load.

Equations to obtain the normalized immittance element values for Chebyshev filters are provided throughout the microwave literature, such as by Bahl [15]. However, using these equations, the element values have been tabulated by Bahl [16] for the convenience of engineers. The tabulated element values are repeated in **Table 4**.

Using **Table 4**, for L_m = 0.2 dB and n = 3, the element values have been obtained, as shown in **Table 5**.

Table 5: Element values of the lowpass filter and corresponding immittances, capacitances and inductances:

k	Element Value	L_k (Henry)	C_k (Picofarad)
0	$g_0 = 1.0000$		
1	$g_1 = 1.2275 = Z_1/Z_0$	1.63×10^{-9}	
2	$g_2 = 1.1525 = Y_2/Y_0 = Z_0/Z_2$		0.611
3	$g_3 = 1.2275 = Z_3/Z_0$	1.63×10^{-9}	
4	$g_4 = 1.0000$		

Notes: Z_0 = 50 Ω and Y_0 = (1/50) mhos.
All element values are normalized to 50 Ω.

The transformation of the lowpass prototype to the desired frequency band and impedance level was achieved by using the following two equations [17]:

$$L_k = g_k(Z_o/2\pi f_1) \text{ for series inductors,}$$

and (5)

$$C_k = g_k(1/2\pi f_1 Z_0) \text{ for shunt capacitors,}$$

where k represents the kth section, L_k is the inductance in Henrys and C_k is the capacitance in Farads. In the first equation, g_k is normalized impedance (Z_k/Z_0) whereas in the second equation g_k is normalized admittance (Y_k/Y_0). These capacitances and inductances are shown in **Table 5**.

Figure 9 illustrates the transformation of the circuit in **Figure 8** to a distributed circuit. The series inductors were replaced by short circuited series stubs and the shunt capacitor was replaced by a shunt open-circuited stub, as shown. Each of these stubs was an eighth of a wavelength long ($\lambda/8$) at the cutoff frequency. This follows the theory of Richard's Transformation, which states that an open-circuited stub that is $\lambda/8$ long behaves like a capacitor while a short-circuited stub that is $\lambda/8$ long behaves like an inductor. [18]

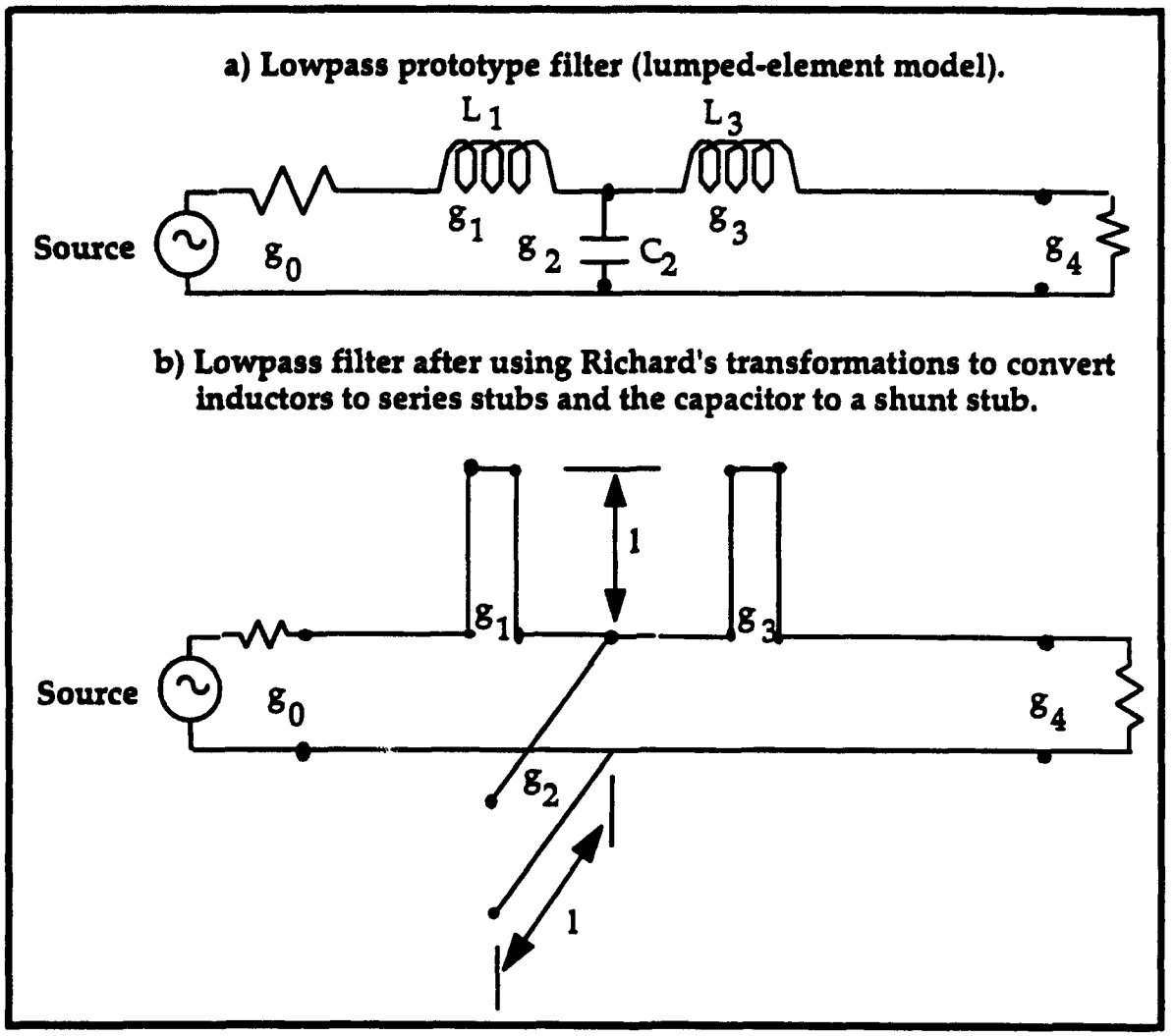

Figure 9: Transformation of lowpass filter to realizable microstrip circuit. (Part 1 of 4)

c) The lowpass filter after adding unit length sections in preparation for use of Kuroda identities.

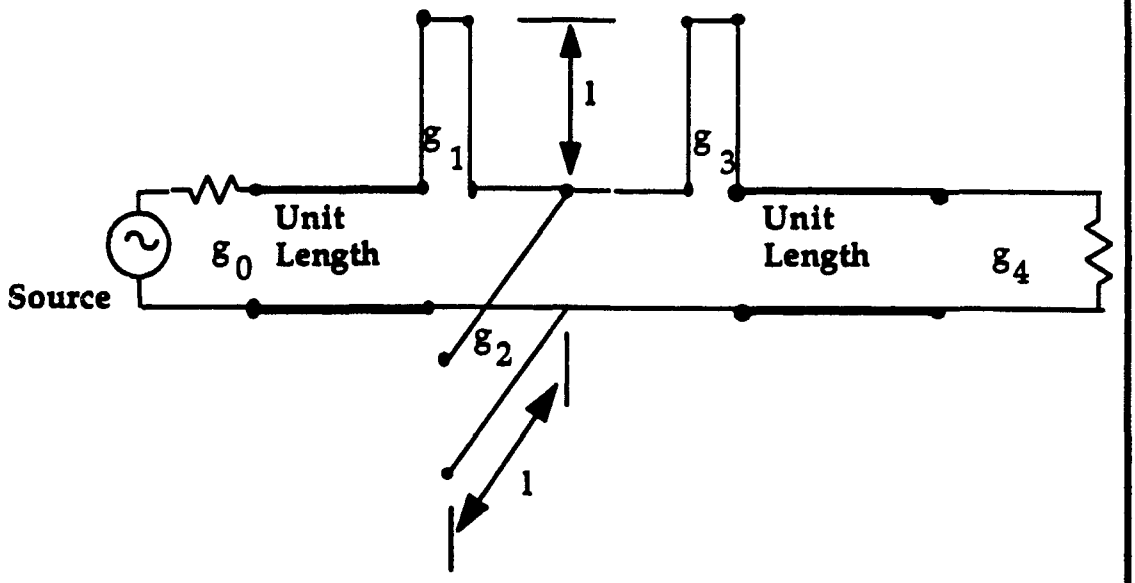

d) Kuroda identity used to transform all series inductive elements to shunt capacitive elements. Z_B represents the normalized impedance of the unit length.

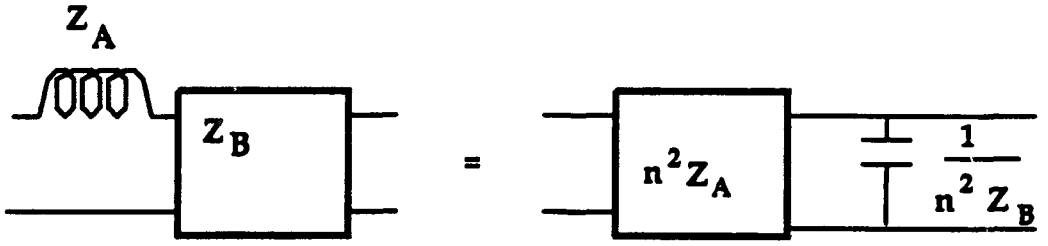

$$n^2 = 1 + Z_B / Z_A$$

Figure 9: Transformation of lowpass filter to realizable microstrip circuit. (Part 2 of 4)

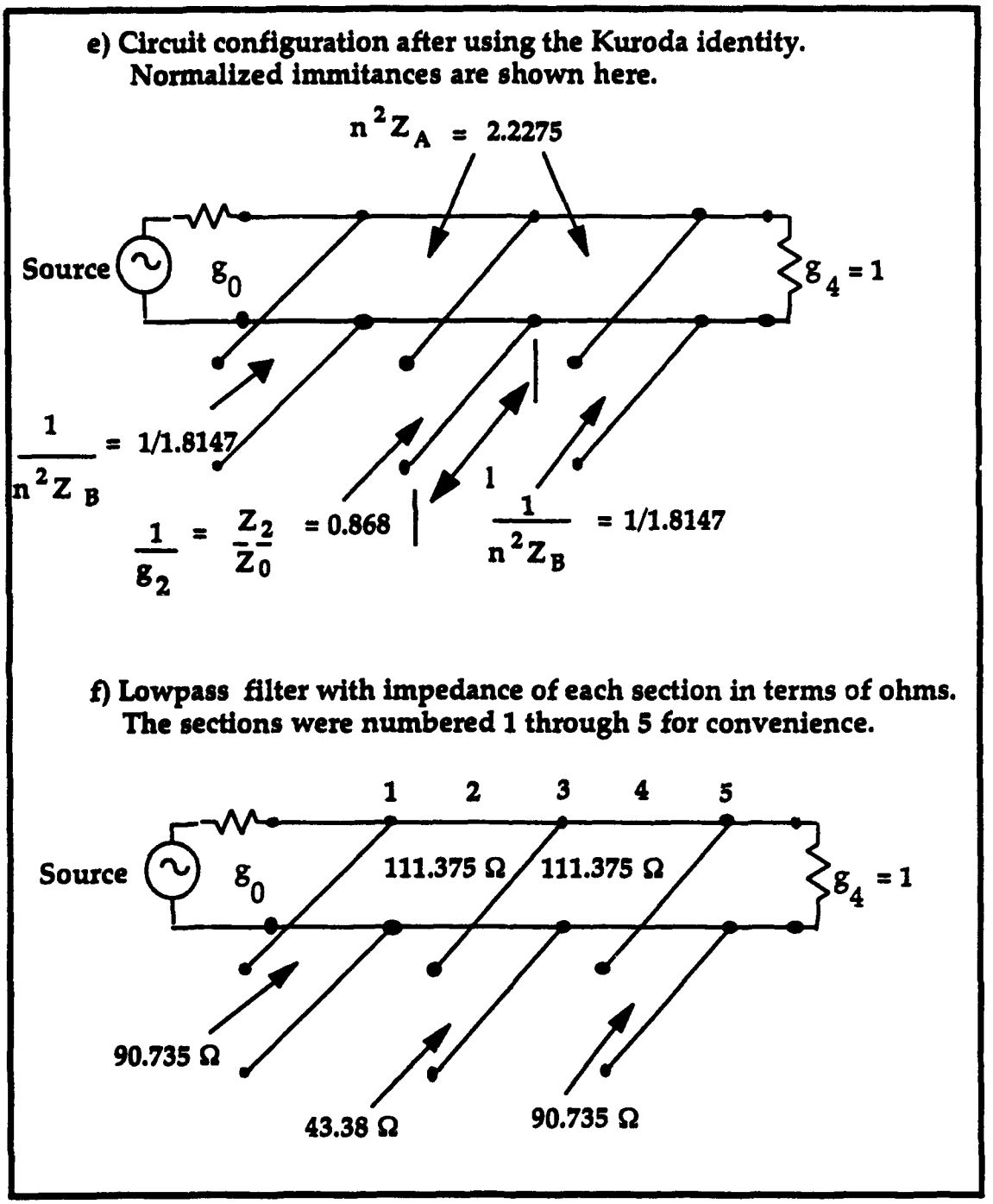

Figure 9: Transformation of lowpass filter to realizable microstrip circuit. (Part 3 of 4)

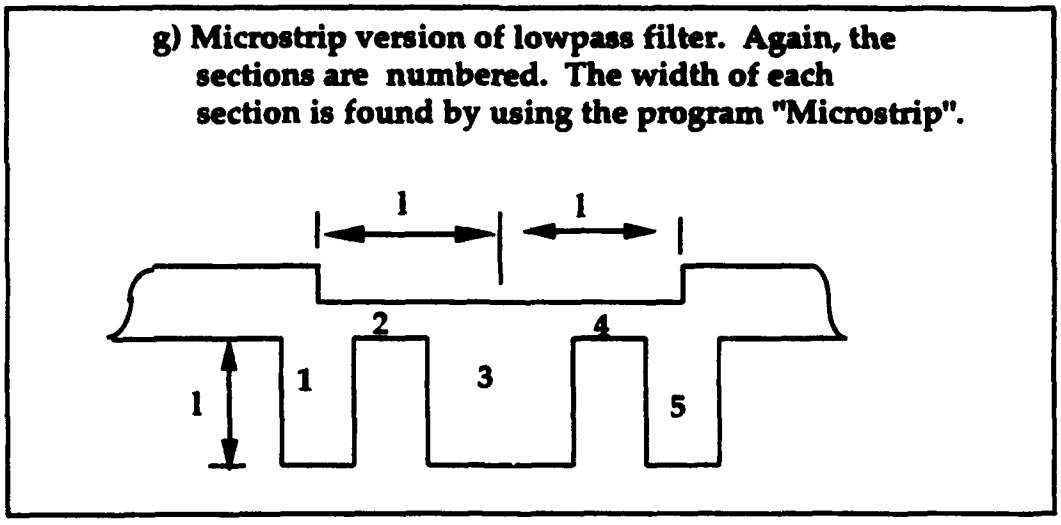

Figure 9: Transformation of lowpass filter to realizable microstrip circuit. (Part 4 of 4)

Series, closed-circuited stubs cannot be realized using microstrip circuits, so it was necessary to use Kuroda identities to convert the series closed-circuited stubs to shunt open-circuited stubs, as outlined by Pozar [19]. First, an eighth-wavelength of 50 Ω line, called a unit length, was placed to the left of the first series stub and another unit length was placed to the right of the second series stub. Then, the Kuroda identity shown in **Figure 9d** was used to convert the series stubs to shunt stubs. This identity converts an inductor in series with a unit length to a transmission line in series with a shunt capacitance.

For the first series inductor, $Z_A = g_1 = 1.2275$ and $Z_B = 1$, since, in the Kuroda identity, Z_B is the unit length impedance. Thus, the identity yields the following calculations:

$$n^2 = 1 + Z_B/Z_A = 1 + 1/1.2275 = 1.8147$$

(Note that n here has nothing to do with number of sections, but refers only to Kuroda identities.)

So the right side of the identity yields:

$$n^2 Z_A = (1.8147)(1.2275) = 2.2275 = \text{normalized impedance}$$

$$1/(n^2 Z_B) = 1/[(1.8147)(1) = 0.5511 = \text{normalized admittance}$$

The resulting circuit is shown in **Figure 9e**. **Figure 9f** shows the same circuit with the impedance value of each section. The sections were numbered for convenience.

In order to transform the filter to a microstrip circuit, a program called "Microstrip" was utilized. This program, written by an engineer at Fort Monmouth, employs a system of equations described in detail in Appendix A. The parameters that the user enters into "Microstrip" are the circuit board dielectric constant, the dielectric thickness, the height of the metal casing above the circuit board ground, the copper thickness and the design frequency, as illustrated in **Figure 10.** The user can then find either the width of a transmission line for a given impedance or vice versa. The program then provides the values for λ, $\lambda/4$ and $\lambda/8$ along the transmission line in question. A value of 100,000 microns was entered for the height of the casing above the circuit since the circuit was designed with no casing involved, i.e., the case height was essentially infinite. All the values which were entered are shown in **Figure 10.** The resulting dimensions are listed in **Table 6.**

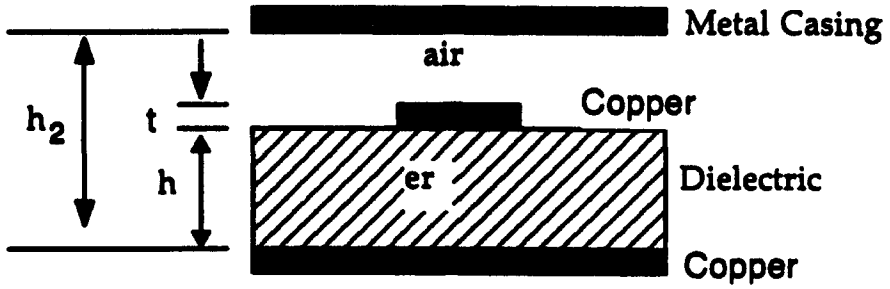

Input Parameters:

er = ε_r = dielectric constant = 2.2
h = dielectric thickness = 787.4 microns
h_2 =height of metal casing above circuit board ground
= 100,000 microns
t = thickness of copper = 12.7 microns
freq = design frequency (= 6.0 GHz = cutoff frequency for lowpass filter)

Two Alternatives Then Open to the User:

1)Enter Z0, where Z0 = characteristic impedance of transmission line.
Obtain the following output parameters: W and λ,
where λ = wavelength along transmission line section and
W = width of transmission line section.

2) Enter W and obtain the following output parameters: Z0 and λ.

Figure 10: Paramters of "Microstrip" program. The value shown for the design frequency is the passband edge frequency for the lowpass filter. The other input parameter values apply to all microstrip sections of the frequency doubler.

Table 6: Dimensions of filter sections resulting from the use of the "Microstrip" program.

Key:
k = section number
Z_k = impedance of kth section
w_k = width of kth section
l_k = length of kth section

k	Z_k, Ω	w_k, μm	l_k, μm
0	50 ohms	2392.1	$\lambda/8$ = 4542.9
1	90.735 ohms	2924.2	l_1 = 4542.9
2	111.375 ohms	1436.2	$l_2 = l_1$
3	43.38 ohms	6009.5	$l_3 = l_1$
4	111.375 ohms	1436.2	$l_4 = l_1$
5	90.375 ohms	2924.2	$l_5 = l_1$

When the lowpass filter was initially designed incorrectly, Kuroda identities were not used.

With L_m = 0.2 dB, f_s/f_1 was chosen to be 6.0/10.0 = 1.7, so the nomograph in **Figure 7** yielded n = 5. The resulting element values are shown in **Table 7**.

The inductors shown in **Figure 11** were mistakenly converted to transmission lines of impedances shown in **Table 7**. This changed a five-pole circuit to a three-pole circuit. The "Microstrip" program was then utilized as shown in **Table 8**.

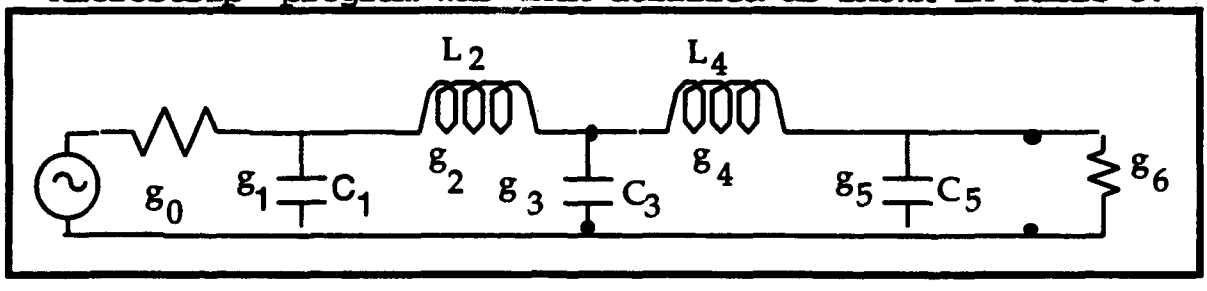

Figure 11: Five-Pole lowpass prototype filter.

Table 7: Element values, immittances, capacitances and inductances for the incorrect lowpass filter. Note that the element values are normalized to 50 ohms.

k	Element Values	Corresponding Immittance	L_k (Henry)	C_k (Picofarad)
0	$g_0 = 1.0$	$Z_0 = 50$ ohms		
1	$g_1 = 1.1468$	$B_1 = g_1/Z_0$ = 0.0229 mhos		0.608
2	$g_2 = 1.3712$	$Z_2 = g_2 Z_0$ = 68.56 ohms	1.82×10^{-9}	
3	$g_3 = 1.9750$	$B_3 = g_3/Z_0$ = 0.0395 mhos		1.05
4	$g_4 = g_2$	$Z_4 = Z_2$	1.82×10^{-9}	
5	$g_5 = g_1$	$B_5 = B_1$		0.608
6	$g_6 = g_0$	$Z_0 = 50$ ohms		

Table 8: Dimensions of filter sections (for incorrect filter) resulting from the use of the "Microstrip" program.

Key:
k = section number
Z_k = impedance of kth section
w_k = width of kth section
lt_k = length of kth section

k	Z_k, Ω	w_k, μm	lt_k, μm
0	50 ohms	2392.1	$\lambda/8 = 4542.9$
1	$1/B_1 = 43.60$ ohms	2924.2	$l_1 = 4542.9$
2	68.56 ohms	1436.2	$l_2 = l_1$
3	$1/B_3 = 25.32$ ohms	6009.5	$l_3 = l_1$
4	68.56 ohms	1436.2	$l_4 = l_1$
5	$1/B_5 = 43.60$ ohms	2924.2	$l_5 = l_1$

In order to isolate the circuit from unwanted dc bias, a chip capacitor placed in series with the lowpass filter was necessary. A 3.3 pF capacitor was available. Since a capacitor in series with a 50 Ω line behaves like a highpass filter with a cutoff frequency f_{HP}, it was informative to find out the cutoff frequency in order to be sure that it was well below the frequencies of operation. This was done as follows [20]:

$$f_{HP} = \frac{1}{2\pi RC} = \frac{1}{2\pi(50\ \Omega)(3.3 \times 10^{-12}\ F)} = 0.965\ GHz \qquad (6)$$

Thus, f_{HP} was much less than the frequencies of interest.

The lowpass filter, including the capacitor, was simulated on a Hewlett-Packard CAD system named "Microwave Design System", or "MDS". The computer drawing of the filter is shown in **Figure 12.** The sections are represented by rectangular boxes separated by zero-resistance wires. Pertinent parameters are listed near each section. Length is designated by L and width is designated by W. The units are microns, designated by um. The lengths and widths are assigned to variables which are defined in the equations above the diagram. On the upper left hand side of the drawing are listed the circuit board dimensions and parameters that were used for this design. For instance, the dielectric thickness is listed as H = 787.4 microns (or 31 mils). The copper thickness T is assumed to be zero, the default value. ER represents the dielectric constant, and COND denotes the default conductivity of the copper.

Using MDS, the filter dimensions were altered slightly until desired simulated results were obtained. For example, the length of the sections was increased until the simulated cutoff frequency was brought down from 8.6 GHz to the desired cutoff frequency. The widths of the stubs were adjusted to decrease the reflections below the cutoff frequency. (The

altered dimensions are shown in **Figure 12**.) These results were plotted on computer and are shown in **Figure 13.** Markers M2 and M4 are on the S21 plot, while marker M1 is on the S11 plot. The frequencies of markers M1, M2 and M4 are designated by I1, I2 and I4 respectively. The power levels are designated by the marker names, i.e., M1, M2, etc.

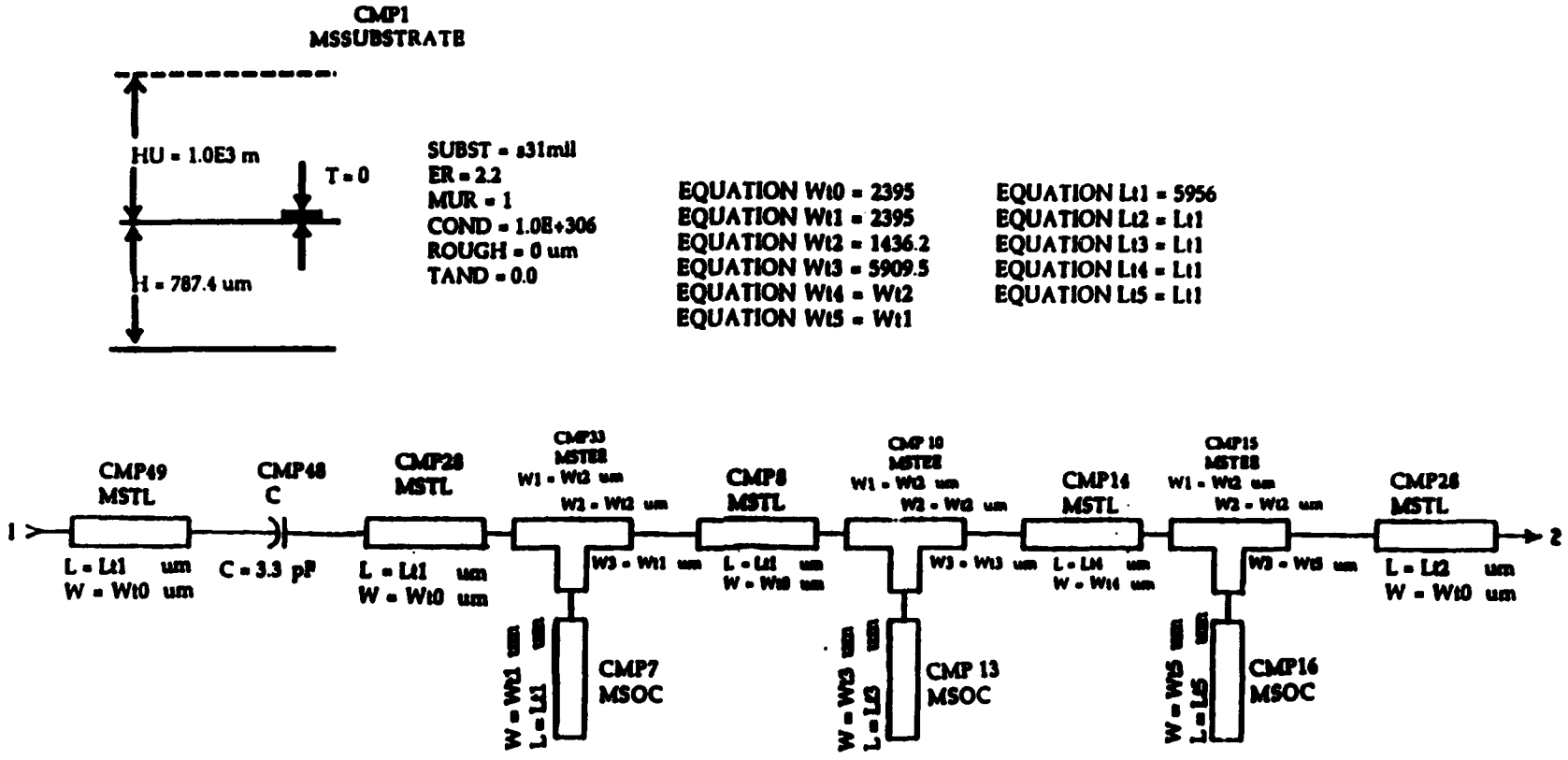

Figure 12: MDS computer diagram of the lowpass filter.

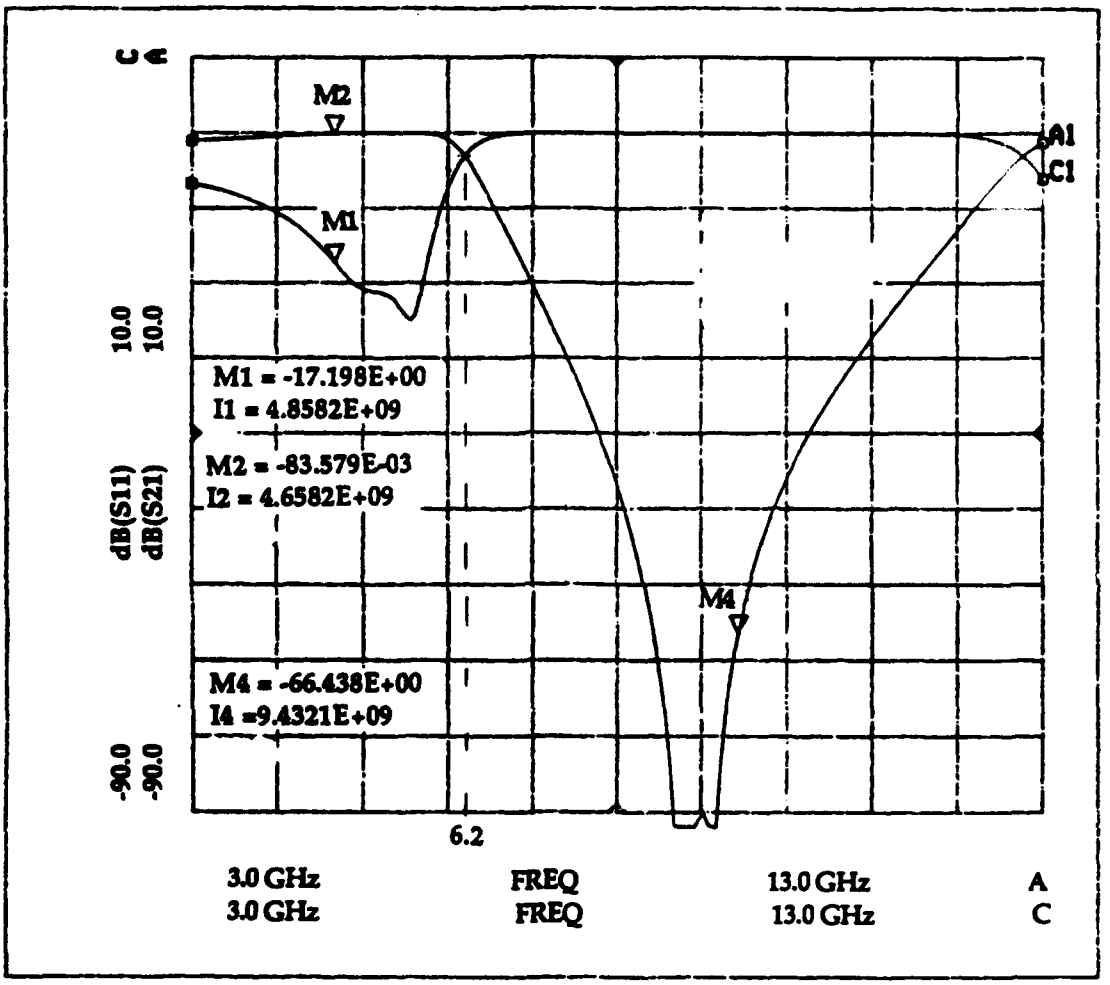

Figure 13: Computer simulated response of the lowpass filter.

Figure 14 gives the dimensions of the actual filter as it was fabricated.

The lowpass filter was etched out of a 31 mil thick circuit board of dielectric constant 2.2. The chip capacitor was soldered in place, and the whole lowpass circuit was mounted onto a brassboard via screws at the four corners. Its photograph is shown in **Figure 15**. The filter was tested on a Hewlett Packard 8510B network analyzer, yielding the results plotted in **Figure 16**. In the plot, S11 is labeled 1 and S21 is labeled 2. **Table 9** compares the desired response, simulated results and actual results.

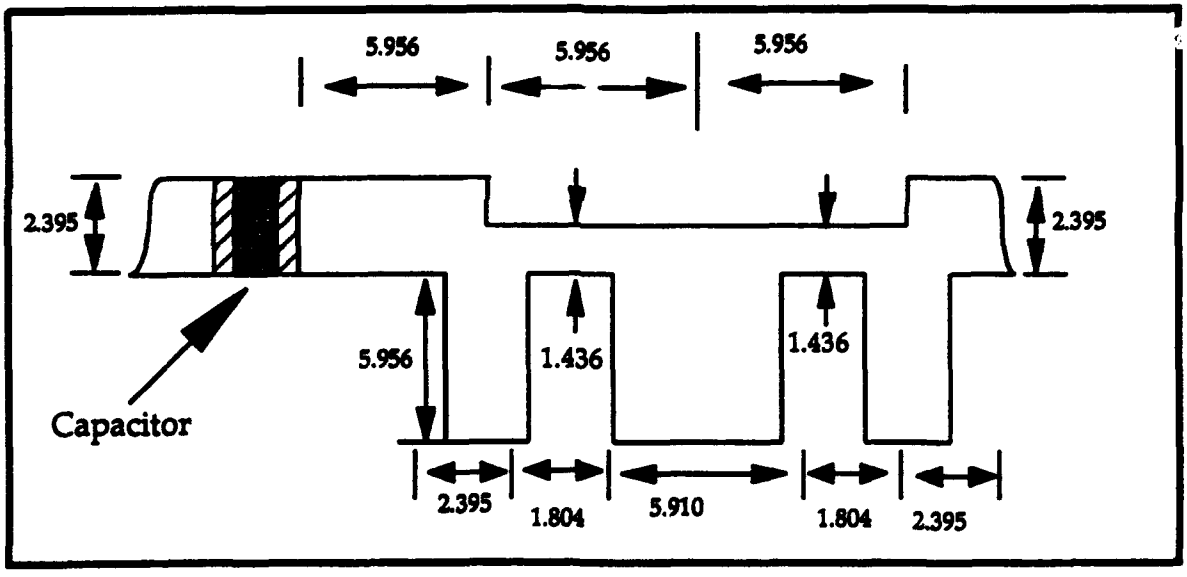

Figure 14: Dimensions of lowpass filter, in millimeters.

Figure 15: Photograph of lowpass filter. The author mistakenly built it with the capacitor on the right side of the filter instead of on the left side. However, so long as the capacitor and filter are in series the same response results.

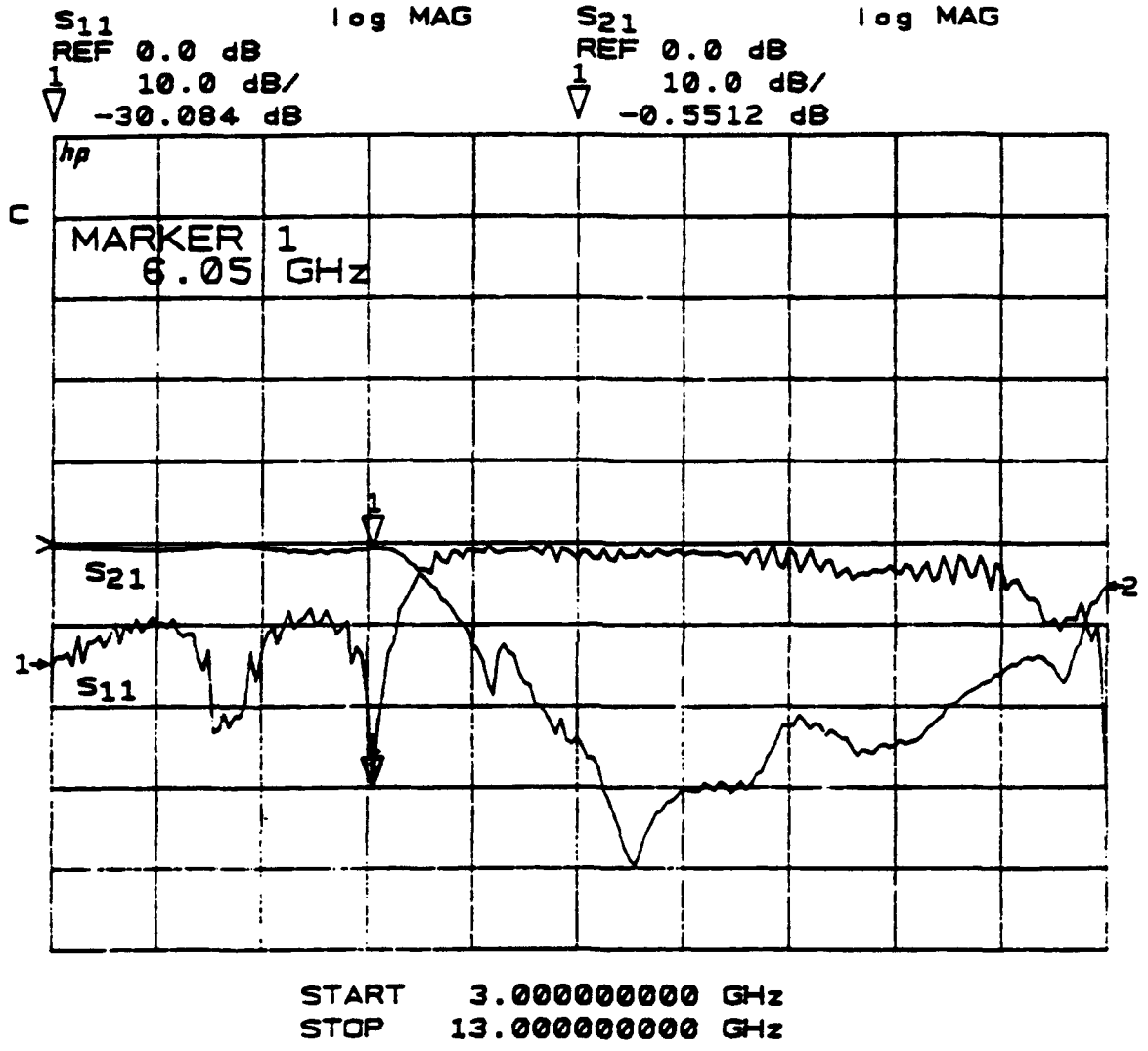

Figure 16: Plot of lowpass filter response.

Table 9: Comparison of desired, simulated and actual results of lowpass filter.

Desired	Simulated
Ripple Factor = L_m = 0.2 dB	L_m = 0
$f_1 = f_c$ = 6.0 GHz	S21 = -3.0 dB @ f_c = 6.2 GHz
f_s = 10.0 GHz	S21 = -30 dB @ f_s = 7.4 GHz
L_s = 30.0 dB	S21 = -66.4 dB @ 9.43 GHz

Actual Results:

L_m = 0.79
@ f_1 = 6.05 GHz, S21 = -1.4 dB and S11 = -8.11 dB
@ f_s = 8.25 GHz, S21 = -29.83 dB: L_s = 29.83 dB
@ f = 9.4 GHz, S21 = -29.70 dB

Output Coupled-Line Bandpass Filter Design

The desired bandwidth for the frequency doubler was 10% of the design frequency. Since the design frequency was 9.4 GHz, the desired output bandwidth was 0.94 GHz. However, as explained by Cohn [21], the actual bandwidth of a coupled-line bandpass filter is always less than the value assumed in the design. Thus, as a rule of thumb, the filter should be designed for a somewhat larger bandwidth than is actually desired. Using the MDS CAD system, several bandwidths were tried until the simulated results were considered reasonable.

The design process, outlined by Bahl [22], is similar to that of a lowpass filter but involves many more calculations.

Figure 17 defines the pertinent design parameters and

compares them with the corresponding lowpass prototype characteristics. [23] [24] As with the lowpass filter design discussed earlier, a Chebyshev response was assumed. Below are listed the design parameters used for the bandpass filter:

L_s = 36 dB
L_m = Ripple Factor = 0.1 dB
f_r = center frequency of passband = 9.4 GHz
f_1 = 8.74 GHz
f_2 = 10.06 GHz
BW = Bandwidth = 1.316 GHz = 0.14 f_r
f_a = edge of lower stopband = f_1 - 1 GHz = 7.74 GHz
f_b = edge of upper stopband = f_2 + 1 GHz = 11.06 GHz

After the design parameters were chosen, ω_s'/ω_1' was calculated as lows [2

$$\frac{\omega_s'}{\omega_1'} = \frac{f_r}{BW}\left[\frac{f_b}{f_r} - \frac{f_r}{f_b}\right] = \frac{9.4}{1.316}\left[\frac{11.06}{9.4} - \frac{9.4}{11.06}\right] = 2.33 \qquad (7)$$

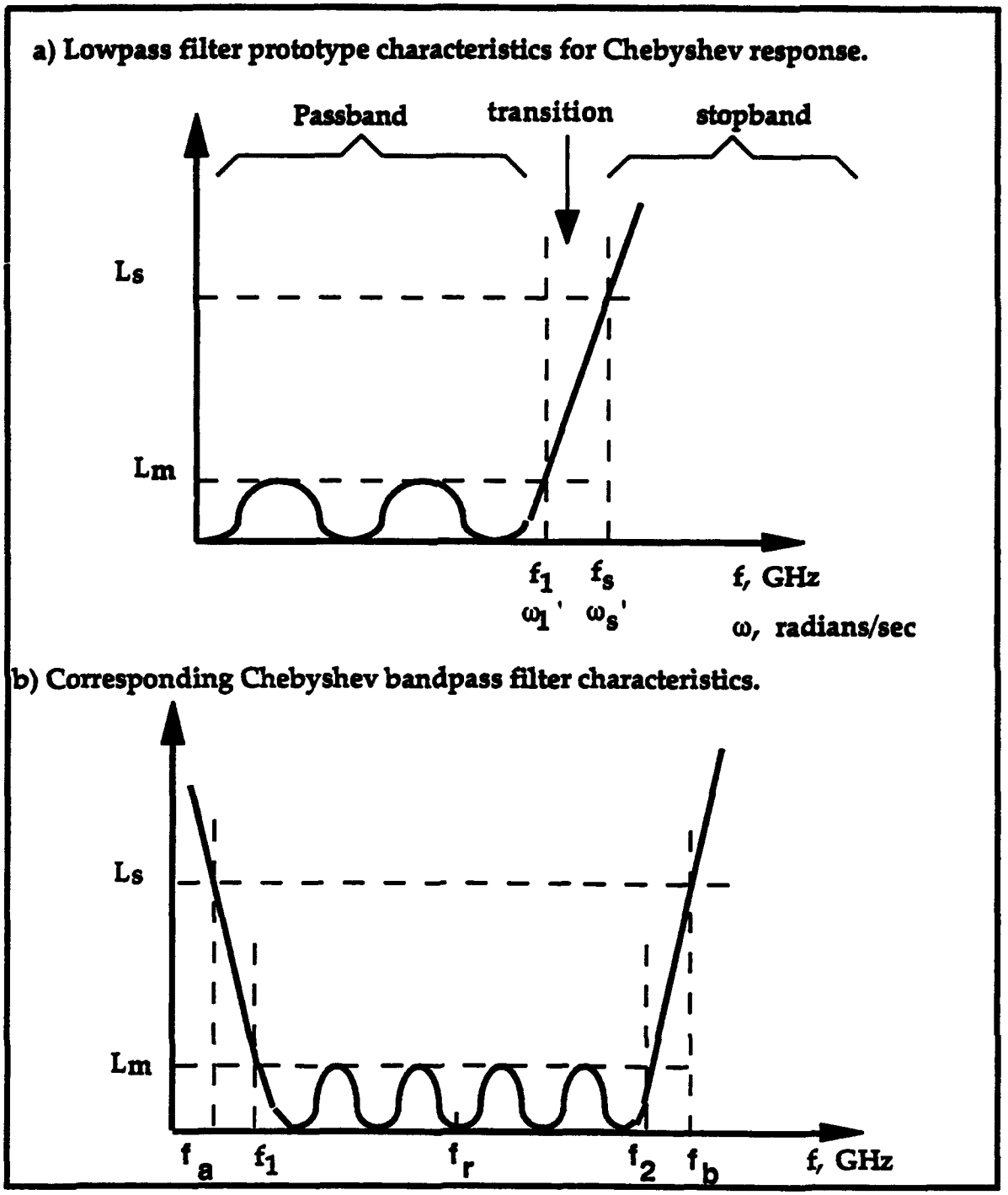

Figure 17: Comparison of lowpass filter prototype characteristics with the corresponding bandpass filter characteristics.

By applying $\omega_s'/\omega_1' = 2.33$, $L_m = 0.1$ dB, and $L_s = 36$ dB to the nomograph in **Figure 7**, the number of sections n was found to be 5. By applying n and L_m to **Table 4**, the Chebyshev element values were obtained, as shown in **Figure 18**.

Figure 18 shows one of several possible lumped-element models of a bandpass filter. [26] The series inductance and series capacitance for the kth section were found from the following two equations [27]:

$$L_k = \frac{g_k Z_0}{2\pi\ BW}, \quad C_k = \frac{2\pi\ BW}{g_k Z_0 \omega_0^2} \tag{8a}$$

where $\omega_0 = 2\pi f_r$. The shunt inductor and capacitor for the kth section were found from the following two equations [28]:

$$L_k = \frac{2\pi\ BW\ Z_0}{g_k \omega_0^2}, \quad C_k = \frac{g_k}{2\pi\ BW\ Z_0} \tag{8b}$$

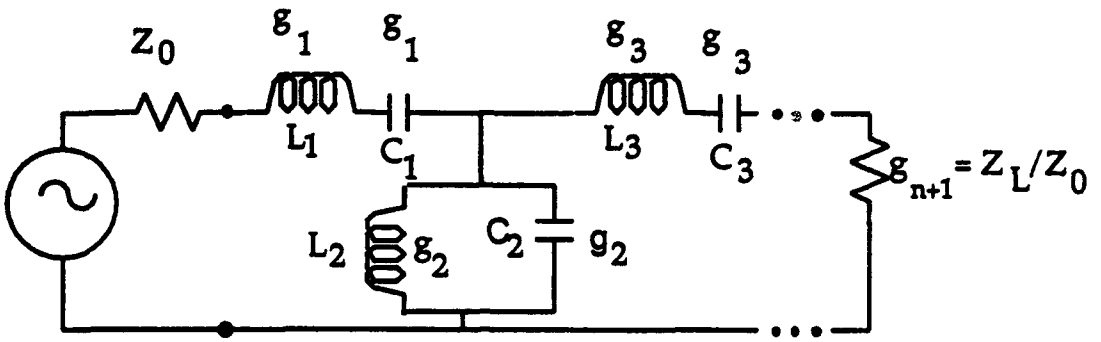

k	Element Values, g_k	L_k (Henry)	C_k (Farad)	Comments
0	$g_0 = 1.0000$			50 ohm line
1	$g_1 = 1.1468$	6.935×10^{-9}	4.134×10^{-14}	Series section
2	$g_2 = 1.3712$	8.644×10^{-11}	3.317×10^{-12}	Parallel section
3	$g_3 = 1.9750$	1.194×10^{-8}	2.401×10^{-14}	Series section
4	$g_4 = 1.3712$	8.644×10^{-11}	3.317×10^{-12}	Parallel section
5	$g_5 = 1.1468$	6.935×10^{-9}	4.134×10^{-14}	Series section
6	$g_6 = 1.0000$			50 ohm line

Figure 18: Lumped element model of bandpass filter. Note that Z_L = load impedance.

Figure 19 illustrates a coupled-line bandpass filter with 5 sections. The length of each resonating section equals a quarter wavelength at 9.4 GHz along a 50 Ω line. Using the Microstrip program, this length was found to be $\lambda/4 = 5781$ μm.

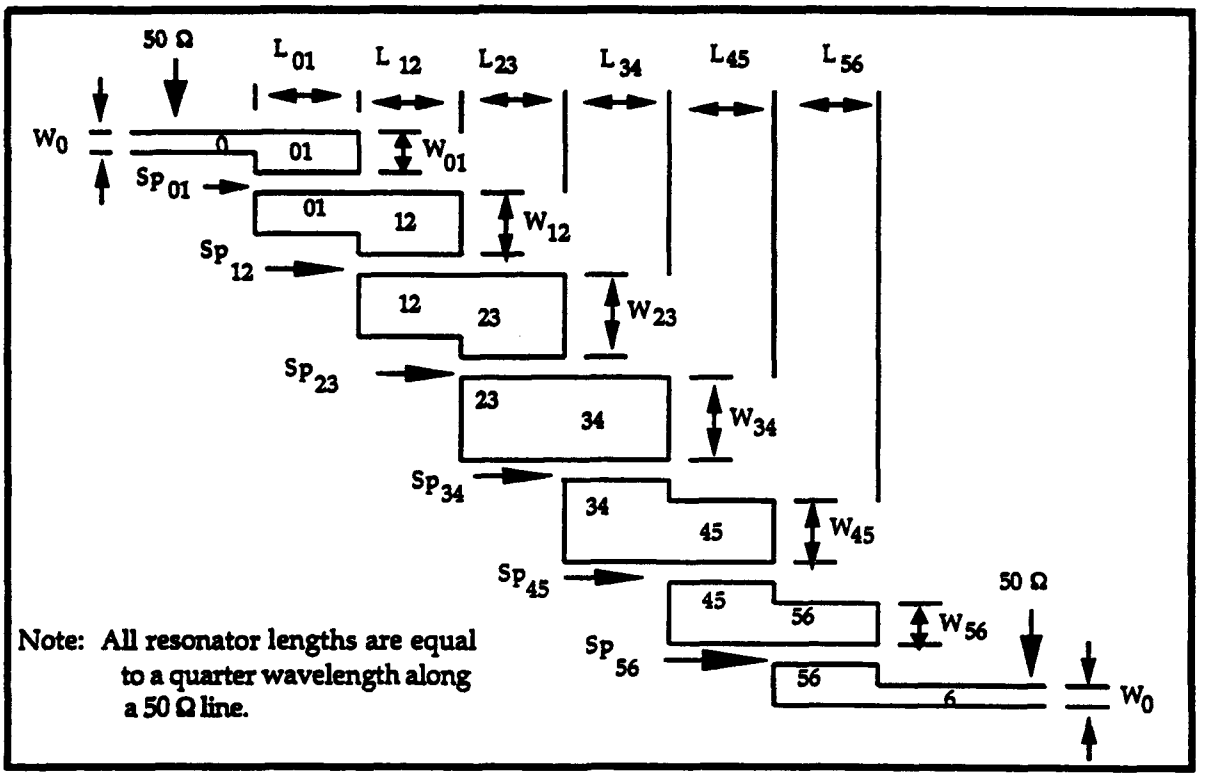

Figure 19: A coupled-line bandpass filter with 5 interior sections.

In order to obtain the desired impedance for each section of the filter, a lengthy group of equations was used. They make use of K-inverters in addition to even-mode and odd-mode impedances in order to find the widths of resonators and the spaces between resonators. These equations are outlined in **Tables 10** and **11. Table 12** summarizes the design parameters derived from these equations.

Table 10: Finding the widths of the resonators of a bandpass filter.

Even and Odd Impedances for Exterior Sections [29]:

$$(Z_{oe})_{01} = (Z_{oe})_{n,n+1} = Z_0\{1 + [1 + (g_1/2)\tan(\phi_1)]^{-1/2}\}$$

and (9)

$$(Z_{oo})_{01} = (Z_{oo})_{n,n+1} = Z_0\{1 - [1 + (g_1/2)\tan(\phi_1)]^{-1/2}\} ,$$

where

$(Z_{oe})_{k,k+1}$ = even impedance of the kth section,
$(Z_{oo})_{k,k+1}$ = odd impedance of the kth section,
$Z_0 = 50\ \Omega$,
$\phi_1 = \pi f_1/2f_r = (\pi)(8.74\,\text{GHz})/[2(9.40\ \text{GHz})] = 1.4605$ radians

Impedance-Inverters for Interior Sections [30]:

$$\frac{K_{k,k+1}}{Z_0} = (\pi/4)(BW/f_r)(1/g_k g_{k+1})^{1/2} \qquad (10)$$

Table 10 (continued):

Even and Odd Impedances of Interior Sections [31]:

$$(Z_{oe})_{k,k+1} = (p)[N_{k,k+1} + (K_{k,k+1}/Z_0)]$$

and (11)

$$(Z_{oo})_{k,k+1} = (p)[N_{k,k+1} - (K_{k,k+1}/Z_0)]$$

where

$$p = \frac{2g_1 Z_0}{2 + g_1 \tan(\phi_1)} \quad (12)$$

and

$$N_{k,k+1} = \{[K_{k,k+1}/Z_0]^2 + [(\tan \phi_1)/2]^2\}^{1/2} \quad (13)$$

Impedance of Each Resonator [32]:

$$Z_{k,k+1} = [(Z_{oe})_{k,k+1} (Z_{oo})_{k,k+1}]^{1/2} \quad (14)$$

This last equation is then applied to the "Microstrip" program in order to obtain the width of section number k,k+1.

Table 11: Obtaining the spacing between resonators [33].

Definition of Variables:

Z_{oe} = even-mode impedance of a given resonator pair.
Z_{oo} = odd-mode impedance of a given resonator pair.
W = width of microstrips in resonator pair.
H = thickness of dielectric of circuit board.
$(W/H)_{se}$ = W/H of a single microstrip transmission line of characteristic impedance $Z_{oe}/2$.

$(W/H)_{so}$ = W/H of a single microstrip transmission line of characteristic impedance $Z_{oo}/2$.

$S_{pk,k+1}$ = spacing between the resonators of resonator pair #k,k+1.

Finding $(W/H)_{se}$:

$$d = \frac{60\,\pi^2}{(Z_{oe}/2)(\varepsilon_r)^{1/2}} \qquad (15)$$

$$(W/H)_{se} = \frac{2}{\pi}(d-1) - \frac{2}{\pi}\ln(2d-1)$$

$$+ \frac{\varepsilon_r - 1}{\pi\varepsilon_r}\left[\ln(d-1) + 0.293 - 0.517/\varepsilon_r\right] \qquad (16)$$

Table 11 (continued):

Finding $(W/H)_{so}$:

$$d = \frac{60\ \pi^2}{(Z_{oo}/2)\ (\varepsilon_r)^{1/2}} \qquad (17)$$

$$(W/H)_{so} = \frac{2}{\pi}(d-1) - \frac{2}{\pi}\ln(2d-1) + \frac{\varepsilon_r - 1}{\pi\varepsilon_r}\left[\ln(d-1) + 0.293 - 0.517/\varepsilon_r\right] \qquad (18)$$

Finding Spacing Divided by Dielectric Thickness (equation 19):

$$\frac{S_{pk,k+1}}{H} = (2/\pi)\cosh^{-1}\left[\frac{\cosh[(\pi/2)(W/H)_{se}] + \cosh[(\pi/2)(W/H)_{so}] - 2}{\cosh[(\pi/2)(W/H)_{so}] - \cosh[(\pi/2)(W/H)_{se}]}\right] \qquad (19)$$

Table 12: Tabulated design parameters of bandpass filter.

k,k+1	$K_{k,k+1}$ / Z_0	$N_{k,k+1}$	$(Z_{oe})_{k,k+1}$ (Ω)	$(Z_{oo})_{k,k+1}$ (Ω)	$Z_{k,k+1}$ (Ω)	$W_{k,k+1}$ (μm)
01	0.3097		70.12	29.88	45.77	2712.9
12	0.0877	4.5160	42.73	41.10	41.9107	3077.8044
23	0.0668	4.5156	42.53	41.29	41.9050	3078.3530
34	0.0668	4.5156	42.53	41.29	41.9050	3078.3530
45	0.0877	4.5160	42.73	41.10	41.9107	3077.8044
56	0.3097		70.12	29.88	45.77	2712.9

(Continued)

k,k+1	$(W/H)_{se}$	$(W/H)_{so}$	$S_{pk,k+1}$ / H	$S_{pk,k+1}$ (μm)
01	5.0681	14.4289	8.16×10^{-4}	0.643
12	9.4808	9.9343	1.105	870.2
23	9.5345	9.8795	1.276	1005.1
34	9.5345	9.8795	1.276	1005.1
45	9.4808	9.9343	1.105	870.2
56	5.0681	14.4289	8.16×10^{-4}	0.643

Notes: Width of a 50 Ω line = W_0 = 2380 μm
Length of Each Resonator = L0 = λ/4 = 5781 μm
On CAD system, L0 was changed to 5305 μm.

Notice in **Table 12** that there is symmetry in the parameters between the first three pairs of resonators and the last three pairs of resonators, as may be expected. Thus, it was only necessary to calculate the the first three parameters.

A comment should also be made concerning the widths of sections 12 through 45. The differences in widths of those sections were smaller than a tenth of a micron. This exceeded the accuracy that was possible in the available fabrication equipment. Thus, their widths were essentially the same.

As with the lowpass filter, this filter was simulated on MDS and the filter parameters were altered until reasonable simulated results were obtained. **Figure 20** is a computer drawing of the circuit along with the modified parameters. Notice that the transition from the 50 Ω line to section 01 (the first pair of coupled resonators) is a taper, instead of the step used in typical coupled-line bandpass filters. A taper is also used between section 56 and the output 50 Ω line. This innovation served the purpose of reducing the reflections and increasing S_{21} in the passband.

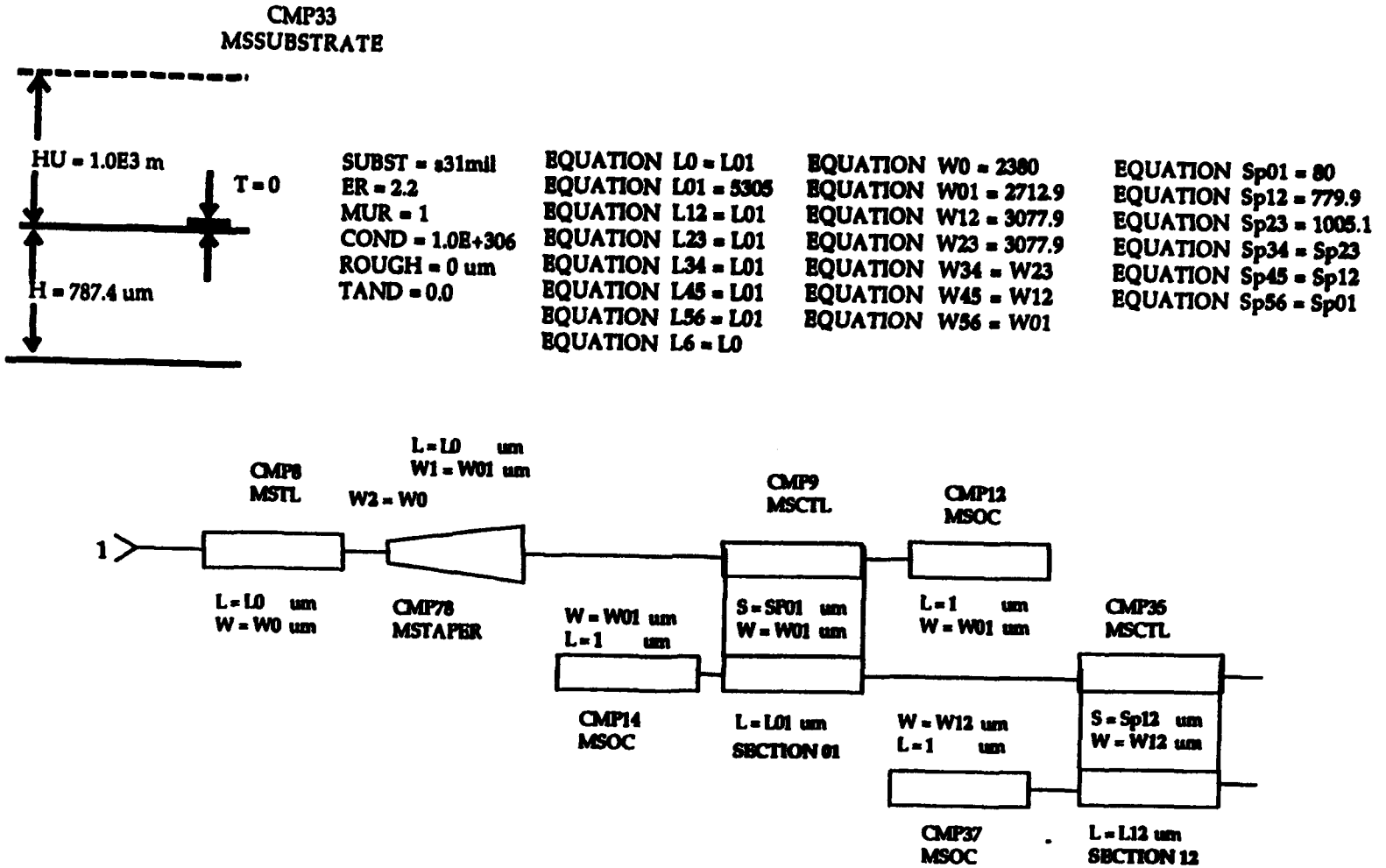

Figure 20: MDS computer drawing of bandpass filter with design parameters listed. (Sheet 1 of 3)

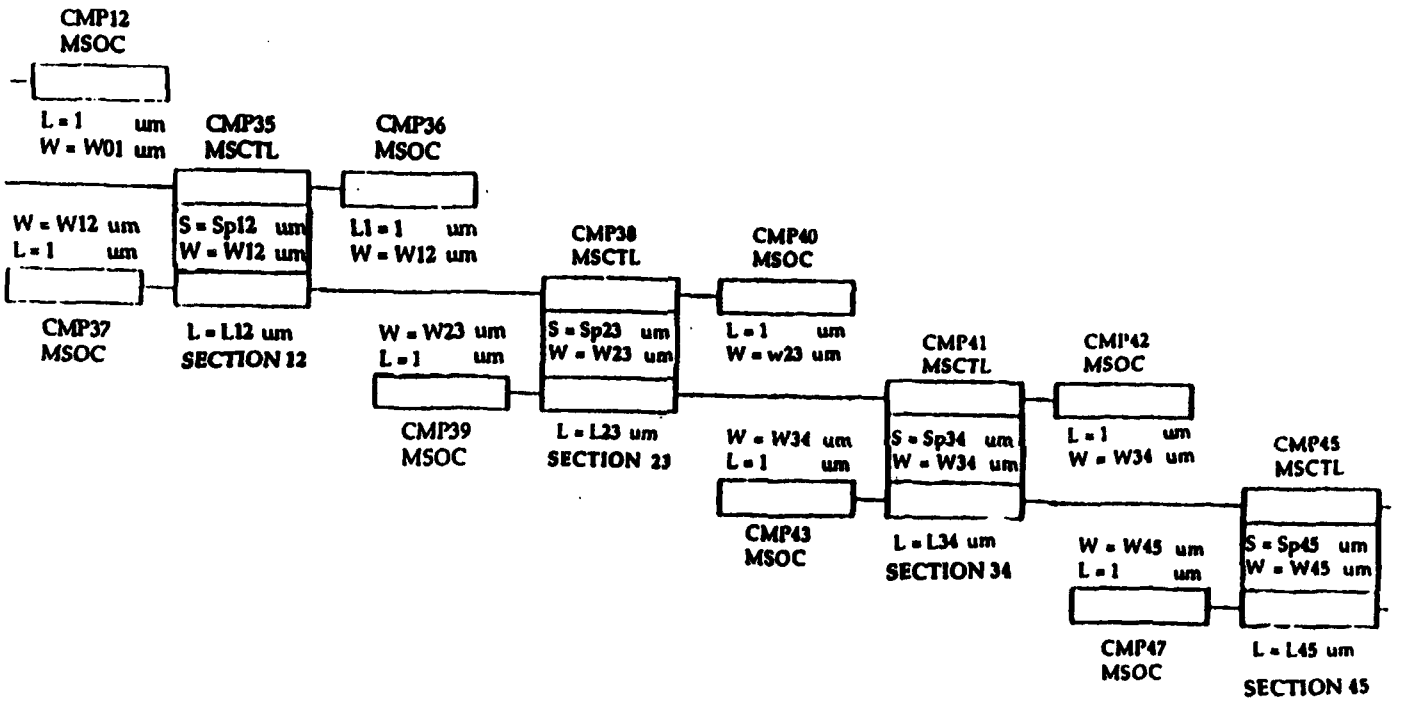

Figure 20: MDS computer drawing of bandpass filter with design parameters listed. (Sheet 2 of 3)

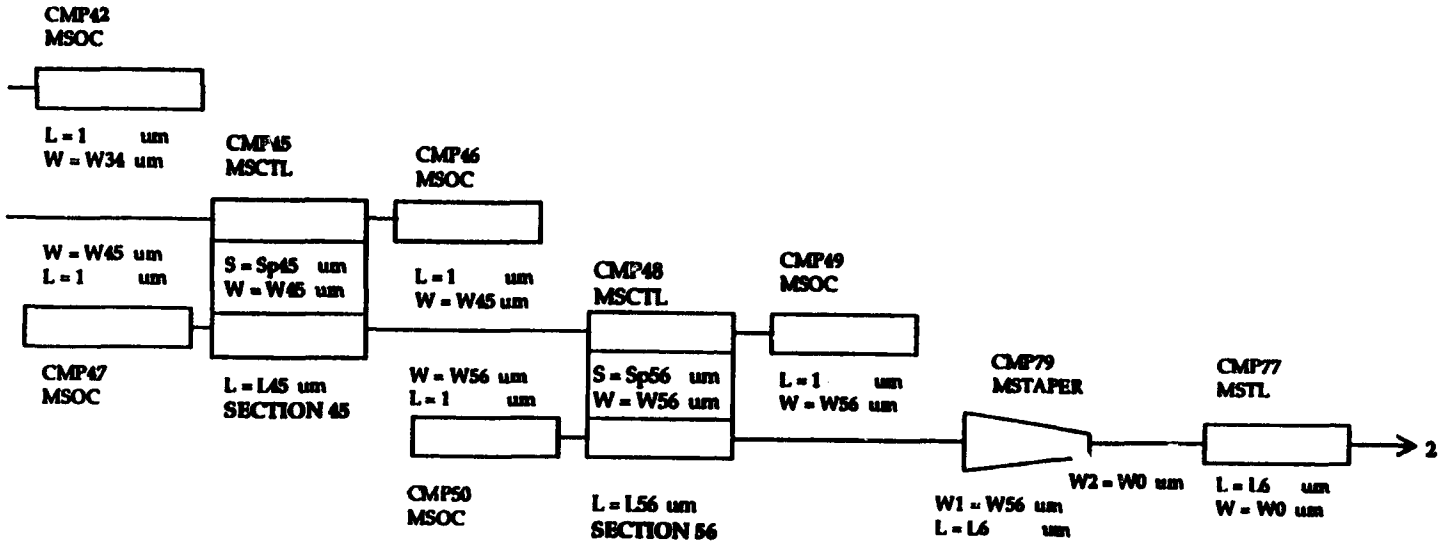

Figure 20: MDS computer drawing of bandpass filter with design parameters listed. (Sheet 3 of 3)

In altering the parameters on the computer model, a couple of rules of thumb were utilized. The first rule of thumb is that the resonant frequency increases as the lengths of the resonators are decreased. The second rule of thumb is that as the spacing between a pair of resonators is decreased, the bandwidth is increased while the ripple factor is decreased.

This second rule of thumb deserves a short discussion. As the space between resonators is decreased, the coupling between the two resonators is improved, thus reducing the ripple factor. Now, suppose a pair of resonators is represented very approximately by a series RLC section. The capacitance C may be treated as a parallel-plate capacitor, where $C = (A\ \varepsilon_{eff}\ \varepsilon_0)/d$, A is the area of the plates (i.e., the area of the facing edges of the resonator pair), ε_{eff} is the effective dielectric constant and d is the space between the resonators. The unloaded quality factor of the RLC section is $Q = 1/2\pi fRC$. If d is decreased, C increases and Q decreases, so the bandwidth increases. Of course, in reality, there is also a capacitance which shunts to ground in the microstrip resonators. But that capacitance remains the same. Only the series capacitance changes, affecting the bandwidth. This simplified model neglects the rest of the surface area of the resonators. However, the same basic principle applies to those surfaces as the space between the resonators is varied. Thus, this highly simplified discussion of a very complicated field interaction is still valid.

The spacings S_{p01} and S_{p56} were too small to be realizable with the equipment available. Another limiting factor was the ability of the computer to model such small spacings. Thus, they were assigned the smallest values which the computer could model, namely, 80 microns.

Figure 21 illustrates the simulated response of the filter. It plots S_{11} and S_{21} in dB versus Hz.

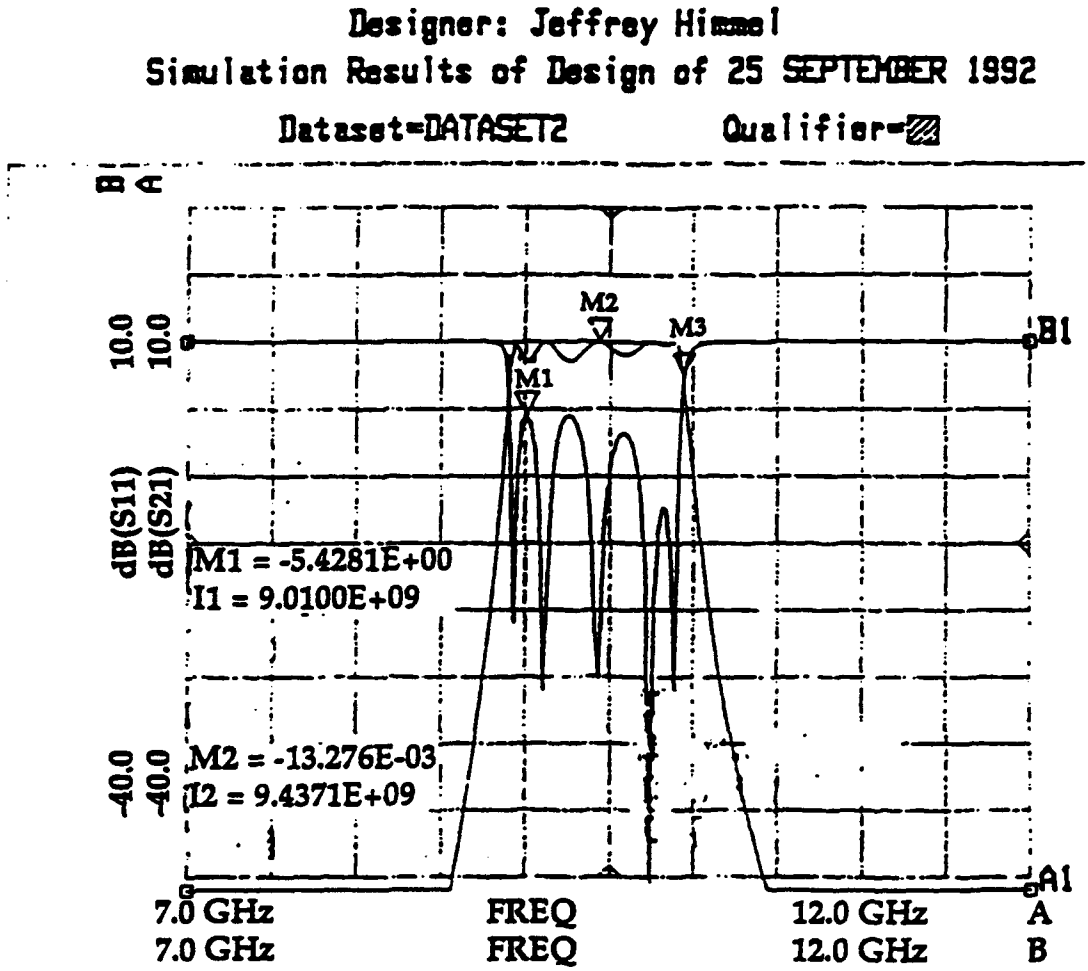

Figure 21: Simulated bandpass filter response in dB vs. Hz.

The bandpass filter was fabricated by the same techniques as the lowpass filter. Its photograph is shown in **Figure 22**. It was tested on the Hewlett Packard 8510B network analyzer, yielding the response shown in **Figure 23**. In **Figure 23**, S_{11} is represented by plot number 1 and S_{21} is represented by plot number 2.

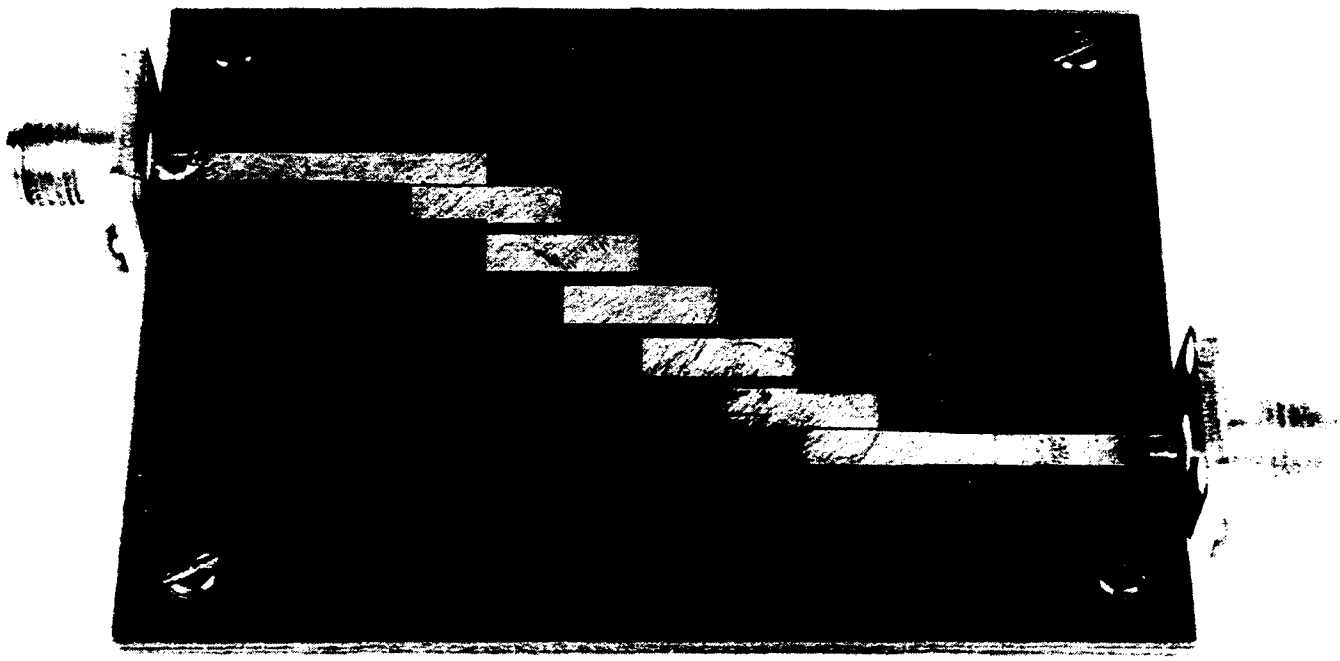

Figure 22: Photograph of bandpass filter.

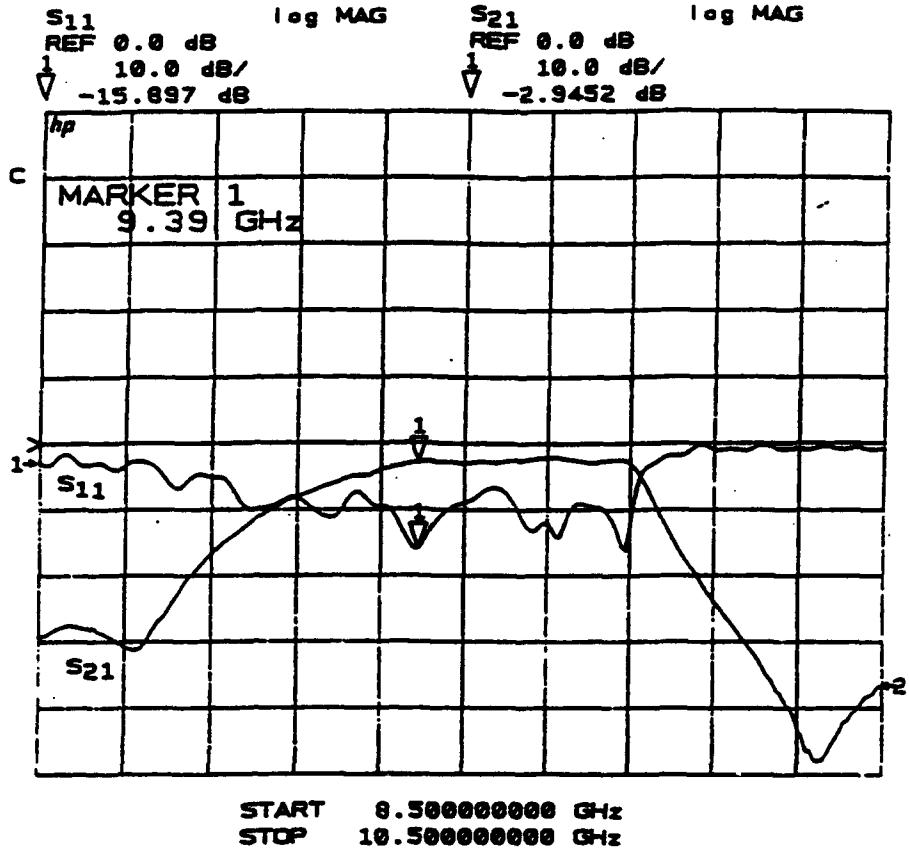

Figure 23: Response of bandpass filter.

Table 13 compares the desired response, simulated response and actual response of the bandpass filter. The ripple factor recorded for each of the three cases is the largest value of L_m. For the actual response of the filter, f_1 and f_2 are defined where the value of S_{21} is 3 dB below that at f_r, thus allowing the determination of the 3 dB bandwidth.

Table 13: Comparison of the desired response, simulated response and actual response of the bandpass filter.

Desired	Simulated
L_a = 36 dB	L_a = 30 dB
L_m = 0.1 dB	L_m = 1.48 dB
f_r = 9.4 GHz	@ f_r = 9.44 GHz, S_{21} = -0.013 dB and S_{11} = -25.15 dB
f_1 = 8.74 GHz	@ f_1 = 8.91 GHz, S_{21} = -2.2 dB and S_{11} = -3.88 dB
f_2 = 10.06 GHz	@ f_2 = 9.94 GHz, S_{21} = -2.50 dB and S_{11} = -3.58 dB
BW = 1.316 GHz = 0.14 f_r	BW = $f_2 - f_1$ = 1.03 GHz = 0.11f_r
f_a = 7.74 GHz	@ f_a = 8.7 GHz, S_{21} = -29.43 dB
f_b = 11.06 GHz	@ f_b = 10.24 GHz, S_{21} = -30.17 dB

Actual

L_m = 0.8 dB
@ f_r = 9.4 GHz, S_{21} = -2.96 dB and S_{11} = -15.04 dB
@ f_1 = 9.17 GHz, S_{21} = -6.40 dB and S_{11} = -11.40 dB
@ f_2 = 9.94 GHz, S_{21} = -6.60 dB and S_{11} = -3.62 dB
3 dB Bandwidth = 0.77 GHz = 0.08f_r
@ f_a = 8.7 GHz, S_{21} = -34.5 dB
@ f_b = 10.24 GHz, S_{21} = -36.1 dB

Design of Diode Section of Frequency Doubler

In the design process of the diode section of the frequency doubler, there were two main concerns, namely, impedance matching and biasing of the diode.

M/A-COM gave typical impedances of the input and output ports of the MA44706 diode. These impedances vary from diode to diode. The input impedance Z_{in} ranges from 5 Ω to 10 Ω, while the output impedance Z_{out} ranges from 40 Ω to 50 Ω. Z_{out} is reasonably close to 50 Ω, so it was initially assumed that impedance matching was unnecessary for the output port of the diode. However, impedance matching was definitely necessary for the input port. Here, it was assumed that Z_{in} was in the center of the range of possible values given, namely, 7.5 Ω.

The technique of designing the impedance matching network is described in detail by Pozar. [34] The network consists of a shunt stub of length l_s at a distance d from the load, as illustrated in **Figure 24**. It is easier to work with admittance when dealing with shunt elements. The distance d is chosen so that the admittance looking towards the load at that distance is $Y_A = Y_0 - jB$, where $Y_0 = 1/Z_0$ and $Z_0 = 50$ Ω. Thus, d matches the real part of the admittance. The susceptance -B is inductive. Thus, to match the imaginary part of the admittance, a capacitive shunt element of susceptance +B is necessary. This is provided by a 50 Ω shunt stub, the length of which is chosen to provide the necessary capacitive susceptance of +B. Thus, with the stub in place, when looking from the stub down the transmission line towards the load, the admittance that is seen is $Y = Y_0 + jB - jB = Y_0$. Using two stubs opposite from each other yields even better results since the stub lengths would turn out to be shorter than that of a single stub. Shorter stubs would make the impedance matching network less frequency sensitive. [35]

The diode was represented by a real load impedance $Z_L = Z_{in} = 7.5\ \Omega$. The frequency which was desired to be delivered to the load was 4.7 GHz. In order to find the wavelength λ at that frequency along a 50 Ω line, the program "Microstrip" was used. The circuit board parameters plugged into the program were the same as with the filters, except that this time the variable freq = 4.7 GHz. Thus, λ = 46445 microns, or 4.6445 cm.

The impedance matching is outlined on the Smith Chart illustrated in **Figure 25**. The normalized admittances and impedances are denoted here with primes. Thus, the normalized load impedance was

$$Z_L' = Z_L/Z_0 = 0.15.$$

The load admittance Y_L' may be found on the Smith Chart opposite Z_L' on the 6.7 SWR circle.

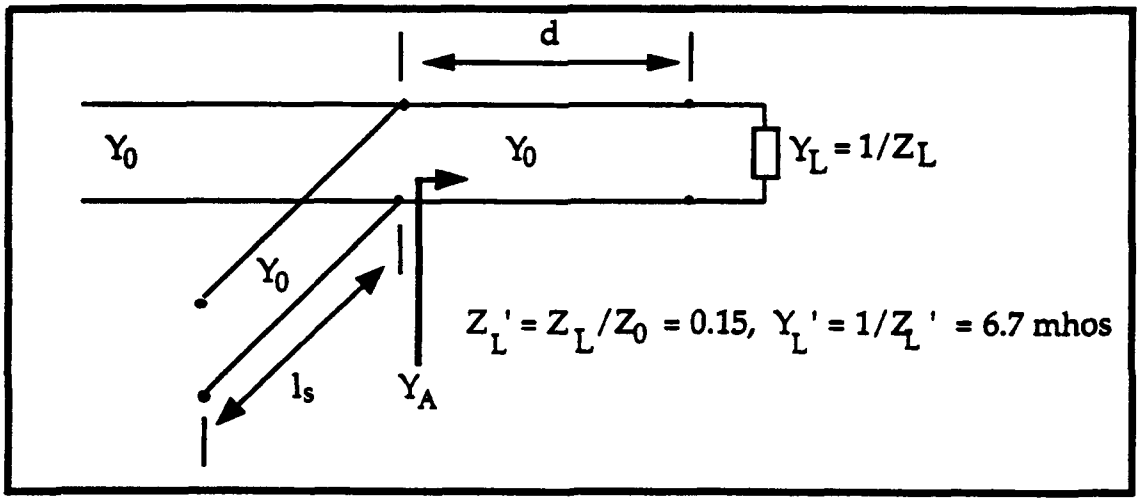

Figure 24: Impedance matching on input side of diode. Note that the load represents the diode.

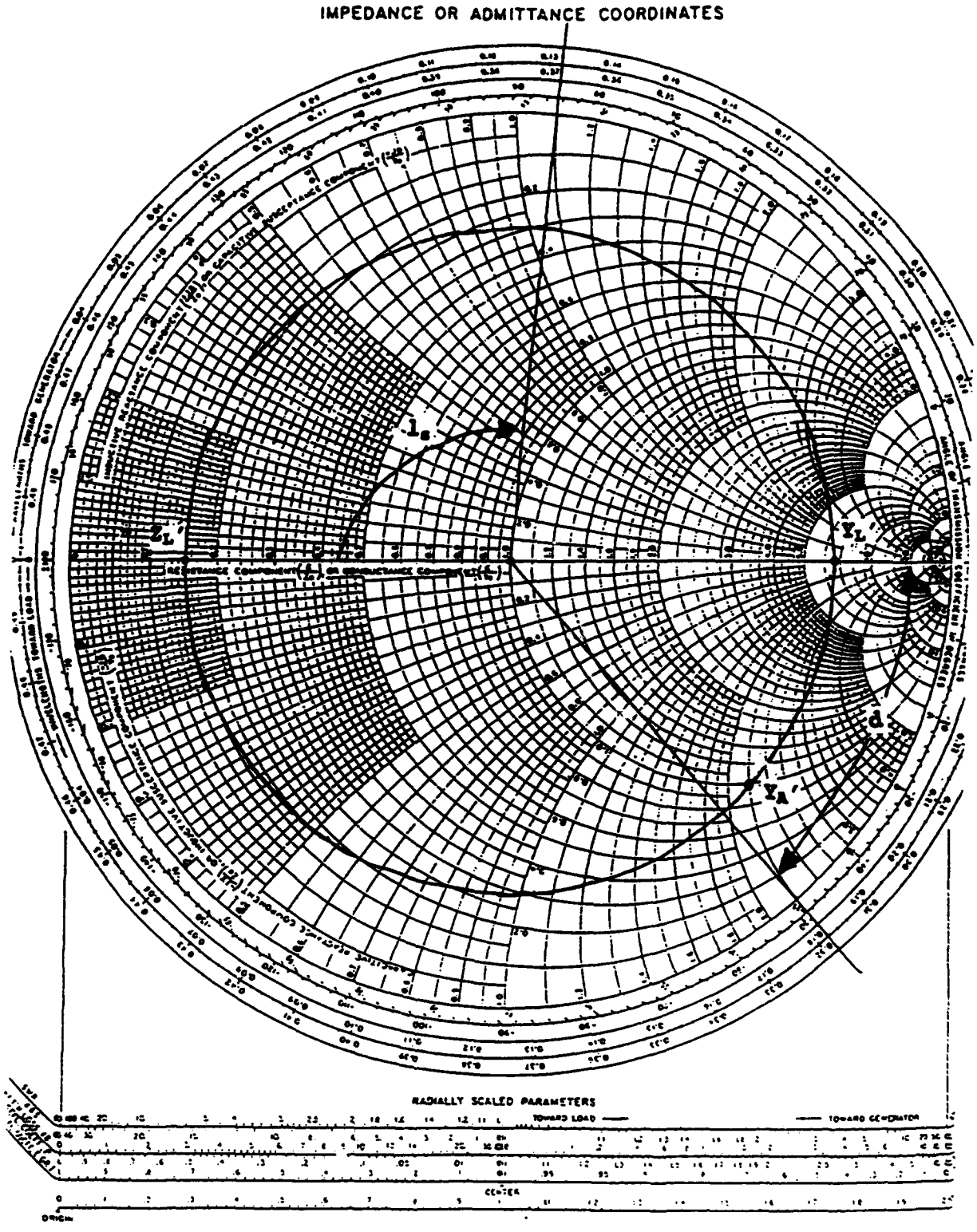

Figure 25: Smith chart used for impedance matching the diode to the circuit.

The distance d was found by moving clockwise towards the generator until reaching the circle of normalized conductance $G' = 1$. That point was labeled Y_A' on the Smith Chart. The distance d was found to be 0.68λ, or 3.1552 cm. From the Smith Chart, $Y_A' = 1 - j2.2$. Thus, a total capacitive stub susceptance of +2.2 was necessary. However, two stubs opposite from each other were used. Recall that total capacitance equals the sum of the individual parallel capacitances. If the total capacitance of the stubs is denoted by C, and the individual capacitances are denoted by C_1 and C_2, then $C = C_1 + C_2$. The total admittance is then $j\omega C = (j\omega)(C_1 + C_2) = j\omega C_1 + j\omega C_2$. $C_1 = C_2$, so the two susceptances are equal. In other words, each stub must provide a susceptance of +1.1. The length of each stub l_s was found by tracing the edge of the Smith Chart from $Y' = 0$ clockwise (towards the generator) to the angle where $B' = +1.1$. ($Y' = 0$ represents the outer edge of each stub, where impedance is infinite.) Thus, $l_s = 0.132\lambda = 0.6131$ cm.

The biasing was accomplished by means of a shunt bias resistor connected to the circuit in such a way as to avoid producing reflections or behaving as an antenna. This was accomplished by using a square pad which was a quarter wavelength on a side. The pad was connected to the circuit by a very narrow line of a quarter wavelength long. This biasing line was located on the output side of the diode at a distance from the diode much less than a wavelength at 9.4 GHz. The basic principle behind this topology is that a wave that leaks from the 50 Ω line to the bias line first sees a very high impedance on the narrow section and then suddenly sees a very low impedance at the quarter wavelength square pad. These sudden changes in impedance reflect most of the power of the waves near 9.4 GHz which attempt to penetrate the bias line. The quarter wavelength dimensions cause the highest amount of reflection at 9.4 GHz since half the wave fits folded on itself within the pad as it is being reflected.

A diagram of the diode circuit is illustrated in **Figure 26.**

An attempt was made to simulate the frequency doubler on MDS. However, the software was unable to simulate the circuit with the output bandpass filter included.

A drawing of the diode circuit is shown in **Figure 27a.** In the fabrication of the diode circuit, a hole was drilled in the brass plate just deep enough and of the right dimensions so that the cathode of the diode can have a snug fit. After the circuit board was etched, a hole just wide enough for the anode was drilled at the desired location on the circuit board in such a way so that the diode was offset slightly from the center of the 50 Ω line. The diode and circuit board were soldered to the brass plate using Indium solder since this type of solder has a low melting point, thus avoiding damage to the diode. The anode was soldered to the circuit board using the usual tin solder, however, since it was only necessary to expose the anode to high temperature momentarily.

Figures 27b, 27c and **27d** are illustrations of the final version of the frequency doubler, as will be discussed in the next section.

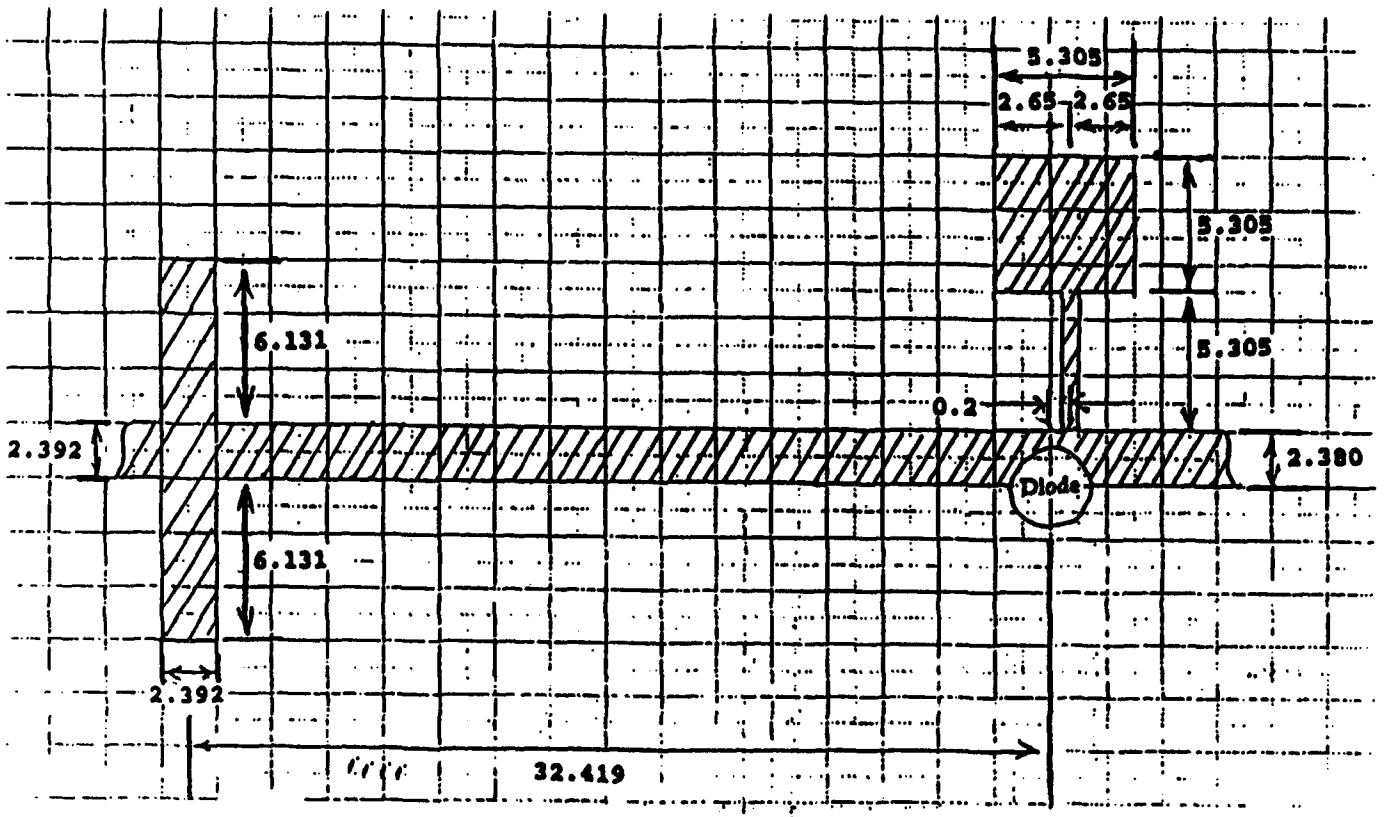

Figure 26: Diagram of diode circuit before tweaking.
(Units are in millimeters.)

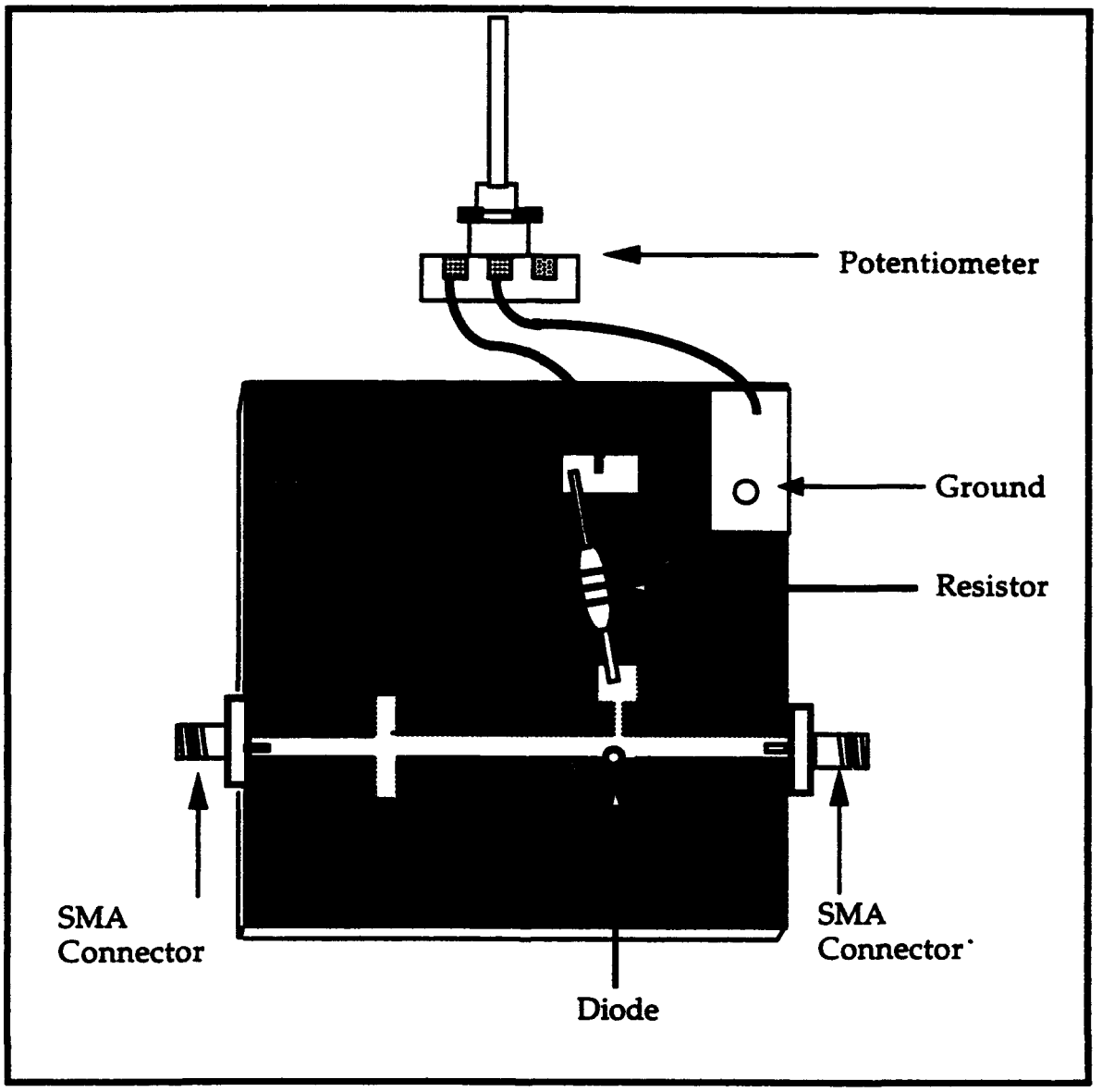

Figure 27a: Drawing of diode circiut in its initial form.

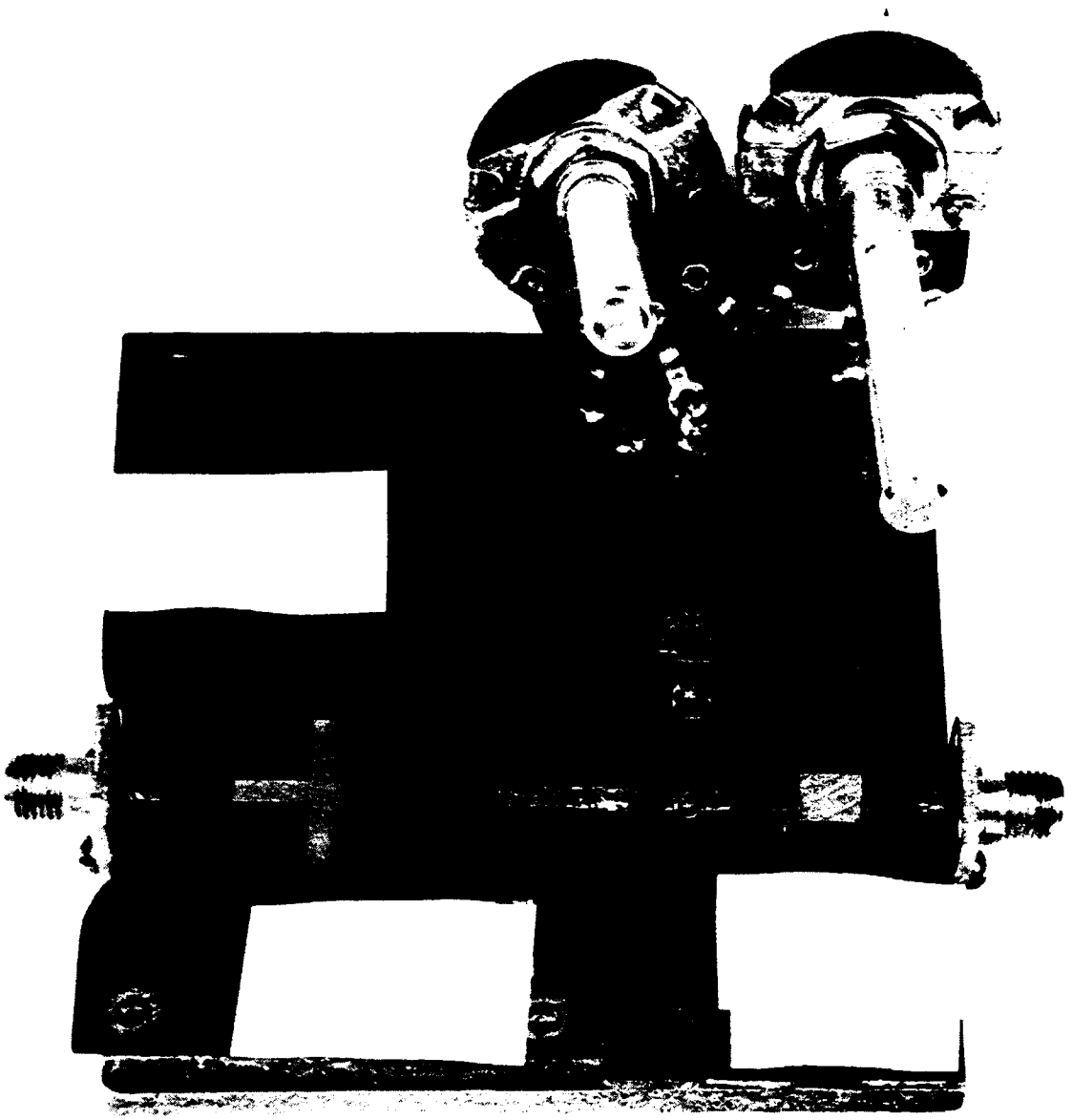

Figure 27b: Photograph of diode circuit in its final form.

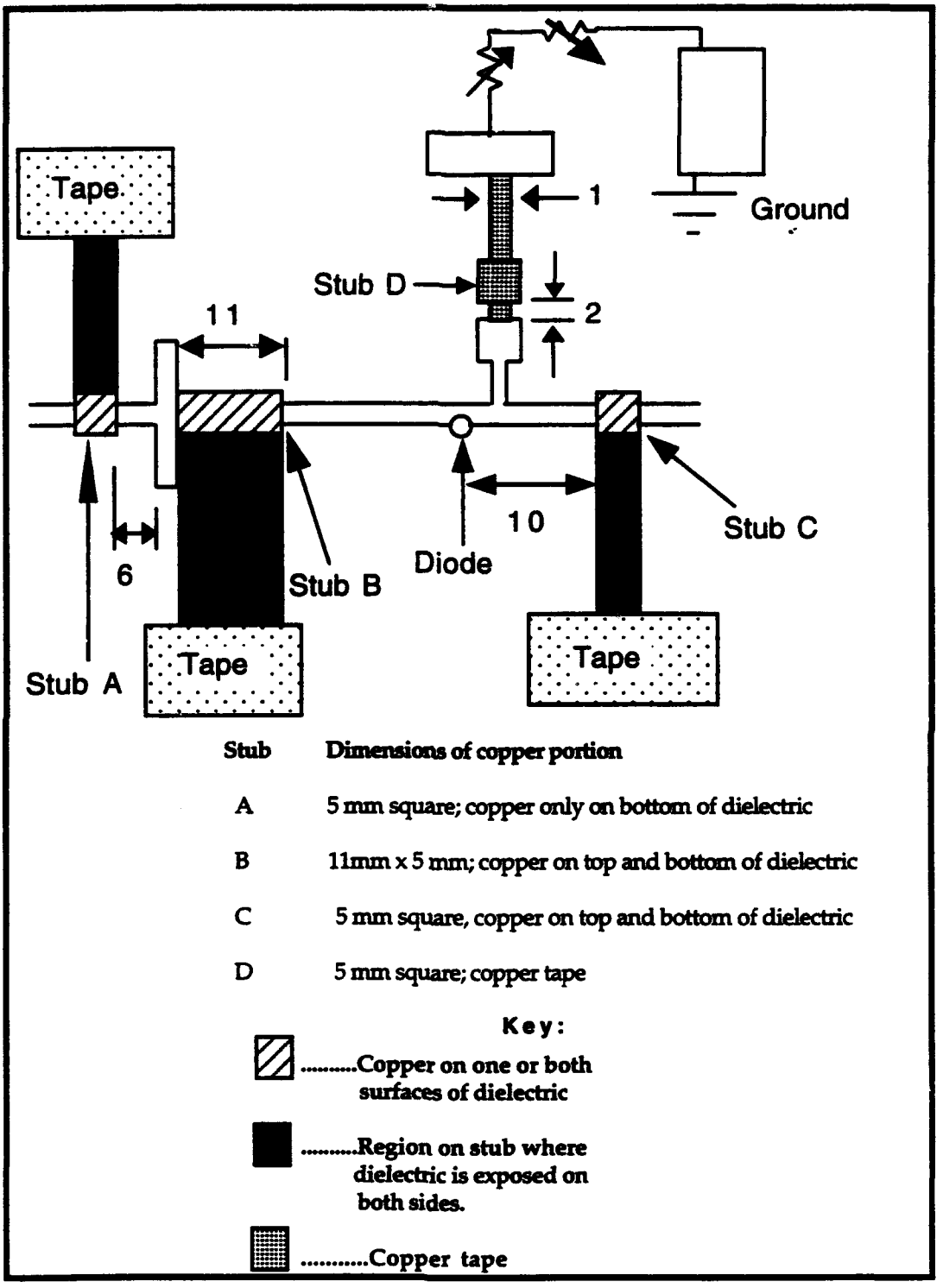

Stub	Dimensions of copper portion
A	5 mm square; copper only on bottom of dielectric
B	11mm x 5 mm; copper on top and bottom of dielectric
C	5 mm square, copper on top and bottom of dielectric
D	5 mm square; copper tape

Key:

.....Copper on one or both surfaces of dielectric

.....Region on stub where dielectric is exposed on both sides.

.....Copper tape

Figure 27c: Diagram of diode circuit in its final form. Locations and dimensions of additional stubs are shown. All units are in millimeters.

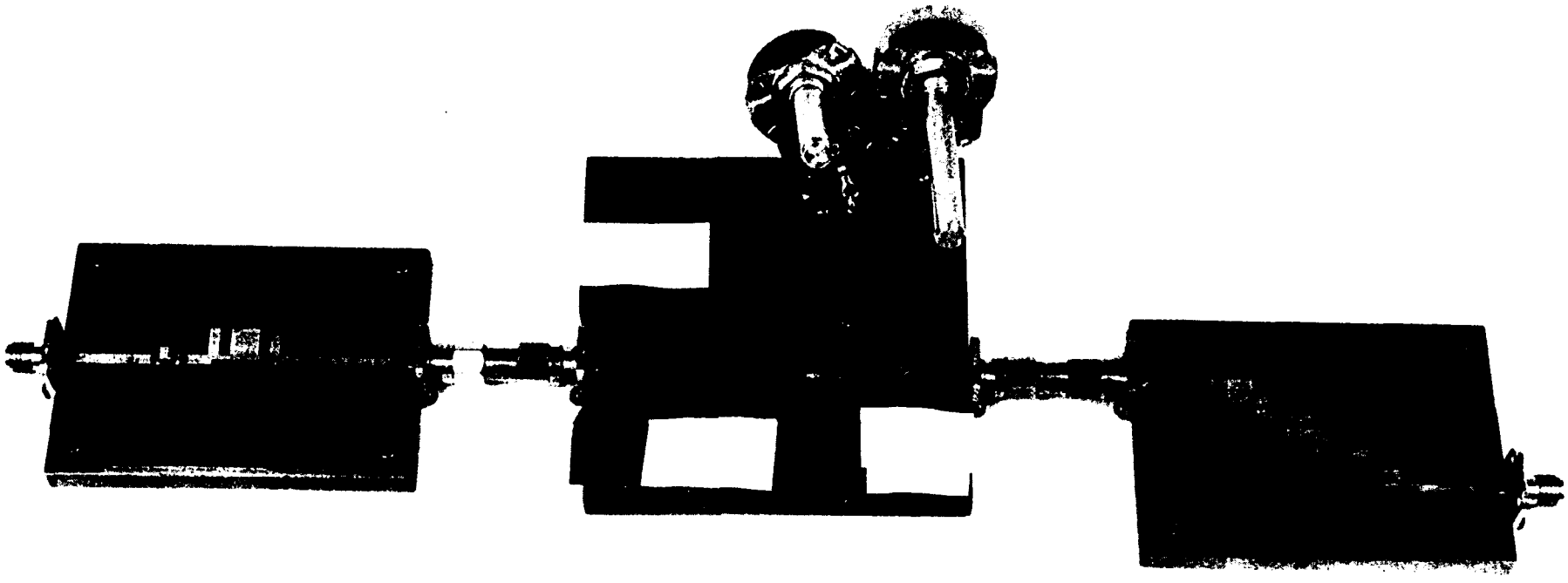

Figure 27d: Entire frequency doubler in its final form.

Results

The three modular sections of the frequency doubler were assembled via SMA adapters. The circuit was tested by using an HP 8340B frequency synthesizer as a source and measuring the output with an HP 8566B spectrum analyzer. After the initial set of results were obtained, the frequency doubler circuit was modified slightly in order to improve its performance.

During the initial set of measurements, when the input frequency was 4.7 GHz, the best efficiency was observed when the input power was 11.0 dBm (12.59 mW) and the bias resistance was set on about 100 kΩ. That efficiency was given by the following equation:

$$\text{Efficiency} = E_{ff} = (\text{Power out})/(\text{Power in})$$
$$= 0.35 \text{ mW} / 12.59 \text{ mW} = .0275, \text{ or } 2.75\ \%.$$

Figure 28 shows a plot of the output frequency response. It is a plot of power (in dBm) and efficiency (in percent) versus frequency. The highest efficiency (5%) occurred at about 9.5 GHz.

In order to improve the efficiency and response, it was necessary to determine where much of the loss was occurring. The input power was 11.0 dBm, while the output power was no higher than -2.0 dBm. That means that the overall loss was at least 13 dBm. Recall that the lowpass filter had an insertion loss of about 1 dB at 4.7 GHz and that the bandpass filter had an insertion loss of about 3 dB at 9.4 GHz. This made it clear that most of the power was being lost in the central diode circuit itself. Two possible sources of loss were investigated, namely, the bias line and the impedance match of the diode to the rest of the circuit.

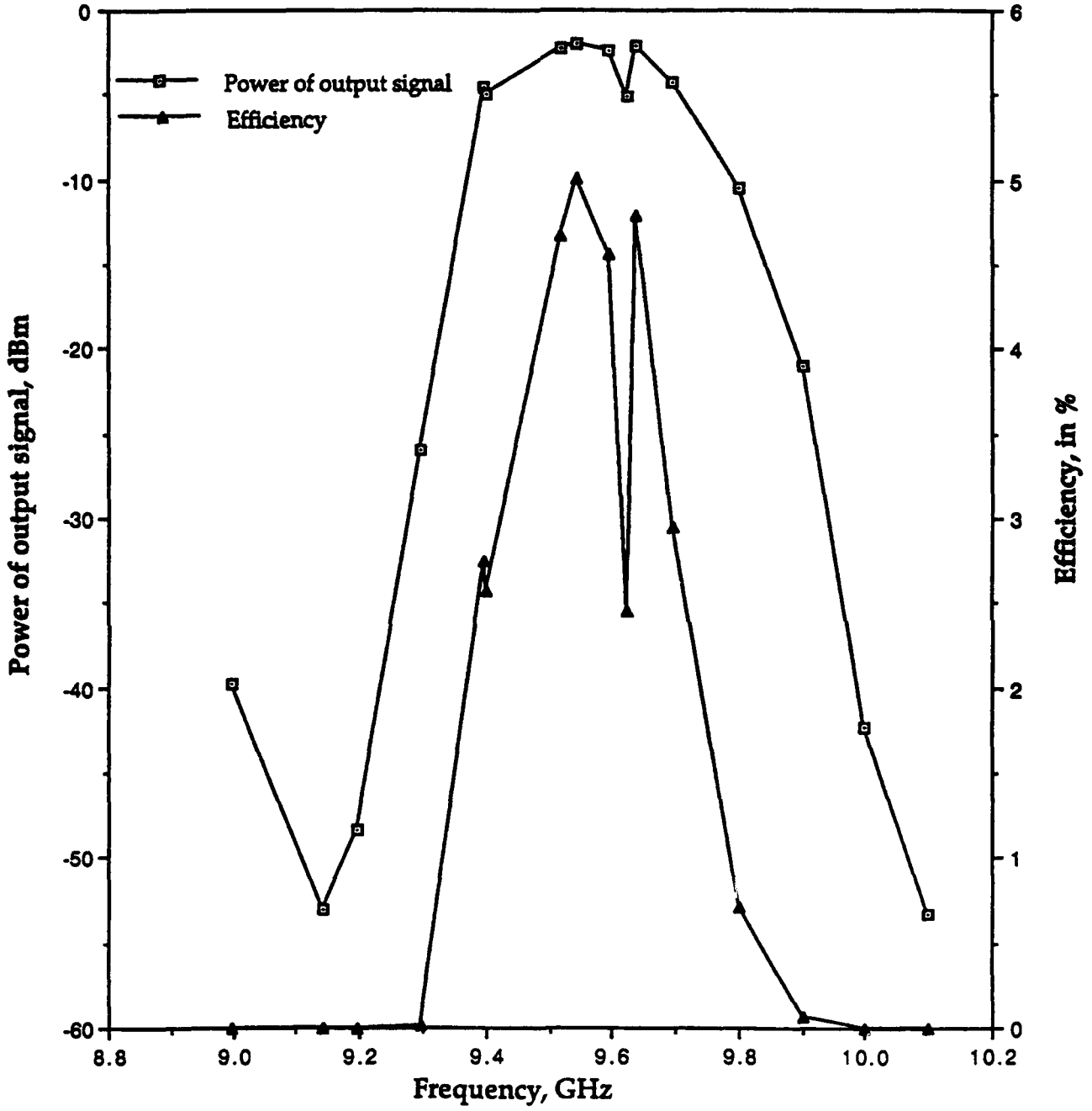

Figure 28: Plot of initial results of frequency doubler.

The bias line initially consisted of a fixed resistor in series with a variable resistor, as illustrated in **Figure 27a**. The fixed resistor was soldered to the square quarter-wavelength bias pad. It was found to have some stray capacitance and/or inductance since if its leads were bent slightly the efficiency of the frequency doubler would change significantly. A similar phenomenon was observed with the wires connecting the variable resistor to the circuit. Any stray capacitance and inductance also undoubtedly had some effect on the frequency response of the circuit. Thus, both resistors were removed. In their place, two variable resistors were put in series without adding lengths of wire to the leads in order to minimize any stray capacitances or inductances. Where the fixed resistor had been, an adhesive copper tape was placed on the circuit board, with one end soldered to the square-quarter-wavelength pad and the other end soldered to one of the rectangular pads (see **Figure 27b** and **Figure 27c**). The width of the copper tape was as small as could be cut (1 mm) in order to have a high impedance. A square piece of copper tape was placed on the narrow adhesive copper line in order to provide some capacitive loading which reflects more of the signal out of the bias line. The dimensions of this piece were 5mm x 5mm, or approximately a quarter wavelength on a side. (The exact dimensions of a quarter wavelength for the tape could not be known due to the unknown dielectric constant and thickness of the adhesive on the bottom of the copper tape.) The edge of the square copper tape was located 2 mm from the original square-quarter-wavelength biasing pad. **Figure 27b** is a photograph of this final form of the diode circuit, and **Figure 27d** illustrates the entire frequency doubler.

The impedance match was improved by cutting out tiny pieces of 31 mil circuit board and using them as capacitive stubs, as shown in **Figure 27c**. Copper was etched away leaving the desired dimensions. First, the input impedance was improved with two stubs, one before and one after the original pair of stubs. Then, the circuit performance was

further improved with a stub to improve the output impedance match. These stubs were taped in place once their optimum locations were found by trial and error. The dimensions of these stubs were empirical.

The results of the modifications are tabulated and plotted in **Figures 29a** and **29b**, respectively. Notice that the highest efficiency was now 13.8% located at 9.4 GHz. Thus, not only was the efficiency improved, but the frequency response was also improved.

Commercially available frequency doublers tend to have efficiencies of about 6%. Thus, the useful passband may be defined as that region of the response in which most of the efficiencies exceed 6%. With this definition, the useful passband of the frequency doubler ranges from 9.35 GHz to 9.8 GHz. This means the bandwidth is about 0.45 GHz. The typical efficiency in this defined passband was found approximately by averaging the measured efficiency values in the passband. Thus, the typical efficiency was found to be 8.31%.

In future frequency doublers, a few improvements in the design and fabrication may improve the circuit behavior. First, instead of taking the manufacturer's word on the input and output impedance of the diode, if time permits, it may be wise to initially build a diode circuit for the sole purpose of measuring the input and output impedances. This minimizes the need for extra tuning ("tweaking") stubs which may have undesirable effects on the frequency response, such as the "valleys" in the passband. Second, all filters may be less lossy if they are soldered to the brass plate, instead of just bolted down, since this eliminates air gaps between the circuit board and the brass plate. Such air gaps cause unknown capacitances which may alter the frequency response. A third improvement is to place two chip capacitors on the central diode circuit, one located before the input impedance matching network and the other after the output impedance

matching network. This would facilitate any desired testing of the diode section without the filters by isolating it from dc.

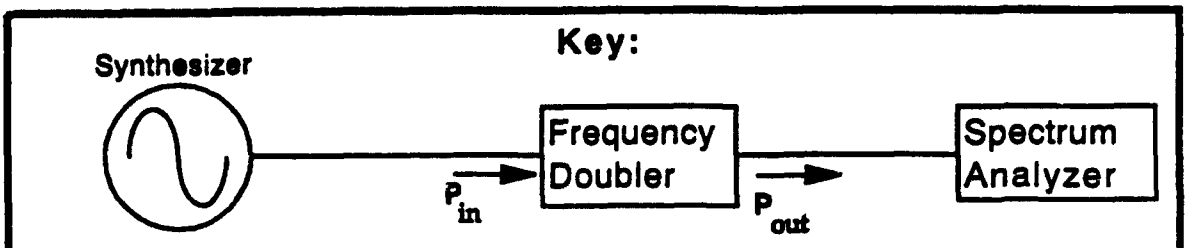

P_{in} = power of input signal

P_{out} = power of output signal at the doubled frequency (first harmonic).

E_{ff} = efficiency of the frequency doubler

Fundamental Frequency, (GHz)	Output Signal Power at Fundamental (dBm)	Doubled Frequency (GHz)	P_{in} (dBm)	P_{out} (dBm)	E_{ff} (%)
4.444	-33.0	8.892	11.0	-28.9	0.13
4.500	-34.0	9.000	11.0	-12.4	0.46
4.548	-38.0	9.100	11.0	-6.1	1.90
4.572	-38.0	9.144	11.0	-3.3	3.72
4.584	-38.0	9.166	11.0	-2.2	4.79
4.600	-37.0	9.200	11.0	-0.5	7.08
4.648	-38.0	9.300	11.0	0.9	9.77
4.676	-38.0	9.350	11.0	1.9	12.30
4.688	-38.0	9.376	11.0	2.0	12.59
4.700	-40.0	9.400	11.0	2.4	13.80
4.724	-38.0	9.450	11.0	2.3	13.49
4.752	-38.0	9.500	11.0	0.8	9.55
4.792	-41.0	9.578	11.0	-1.9	5.13
4.800	-41.0	9.600	11.0	-3.0	3.98
4.812	-41.0	9.622	11.0	-1.7	5.37
4.832	-40.0	9.664	11.0	-4.3	2.95
4.844	-40.0	9.686	11.0	-1.2	6.03
4.860	-40.0	9.722	11.0	-3.2	3.80
4.872	-40.0	9.742	11.0	0.3	8.51
4.900	-40.0	9.800	11.0	0.6	9.12
4.953	-41.0	9.900	11.0	-7.4	1.45
5.000	-41.0	10.00	11.0	-24.4	0.03

Figure 29a: Tabulated results of final form of the frequency doubler.

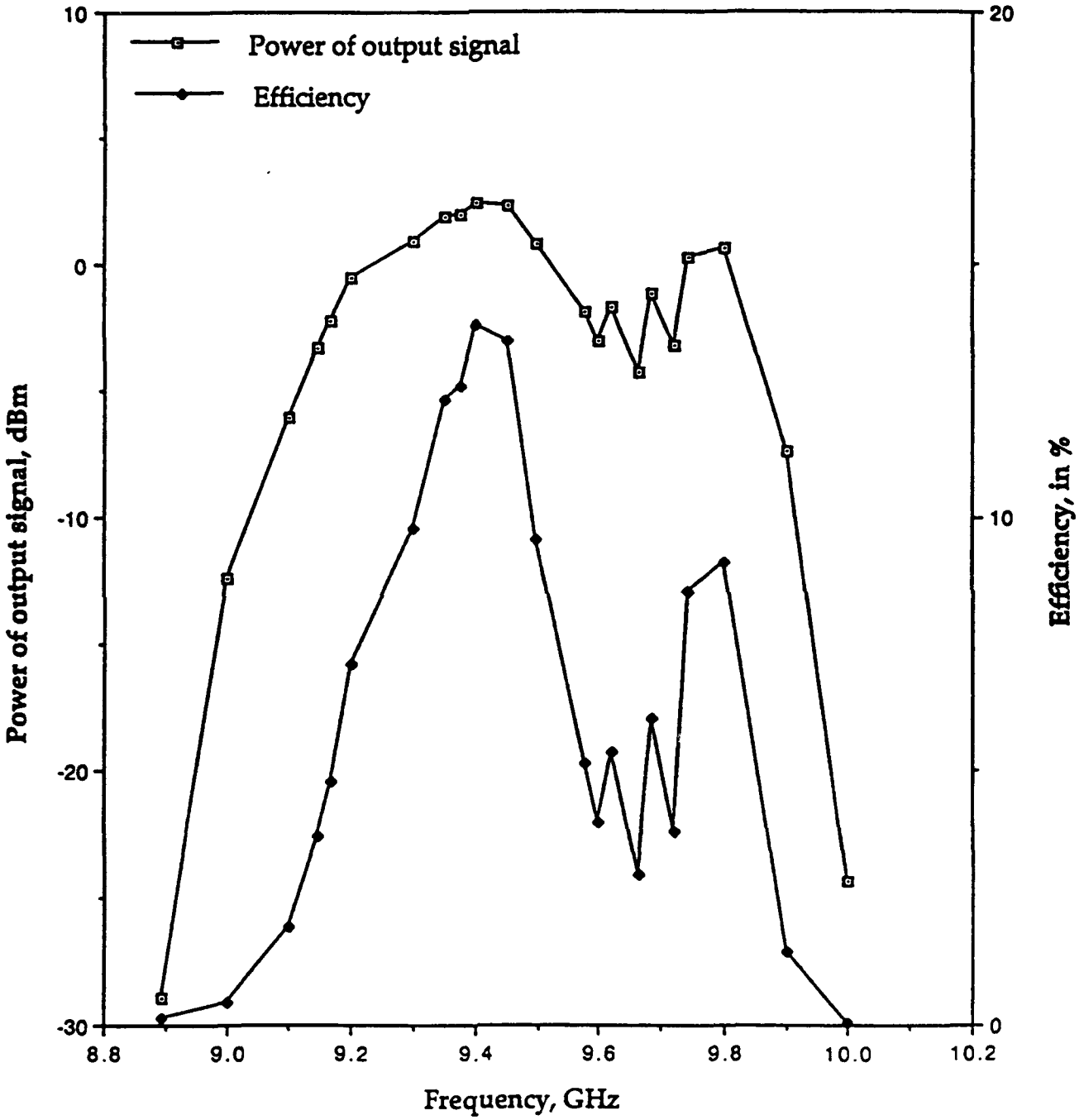

Figure 29b: Plotted results of final version of circuit.

Appendix A: Notes on the Program called "Microstrip"

"Microstrip" is a program which calculates either the characteristic impedance or the width of a microstrip transmission line, depending on what the user specifies. It also corrects the effective dielectric constant ε_{eff} for frequency and provides the wavelength along the transmission line. The program is based on two papers, one written by James J. Lev [36], and the other by M. Kirsching and R. H. Jansen [37].

The program initially requests the user to enter the circuit board dielectric constant, the dielectric thickness, the height of the metal casing above the circuit board ground, the copper thickness and the design frequency, as illustrated in **Figure 9**. It then asks the user whether it is desired to find the impedance or the width of the transmission line. If the impedance is desired, the user enters the width, and vice versa. In either case, the values for the effective dielectric constant, λ, $\lambda/4$ and $\lambda/8$ are provided.

Lev wrote his paper to find some calculated value of impedance Z_{0calc} by comparing it to the required value of impedance Z_{0req} through some iterative process which repeats in the program until $Z_{0req} - Z_{0calc} = 0$. Z_{0calc} is found from the following equation:

$$Z_{0calc} = \frac{Z_{0air}}{[\varepsilon_{eff}(f=0)]^{1/2}} \qquad \text{(A-1)}$$

where $\varepsilon_{eff}(f=0)$ is the dielectric constant, assuming frequency is 0, and Z_{0air} is the impedance in an air dielectric. Both ε_{eff} and Z_{0air} are found from the following system of equations:

$$Z_{0air} = Z_{0air_\infty} - \Delta Z_{0air} \qquad \text{(A-2)}$$

where

$$Z_{0air_\infty} = 60 \ln \left[\frac{f(w/h)}{w/h} + [1 + (2h/w)^2]^{1/2} \right] \qquad \text{(A-3)}$$

$$f(w/h) = 6 + (2\pi - 6)\exp\left[-\left(\frac{30.666}{w/h}\right)^{0.7528}\right] \qquad \text{(A-4)}$$

$$\Delta Z_{0air} = PQ \qquad \text{(A-5)}$$

$$P = 270\left\{1 - \tanh\left[1.192 + 0.706(1 + h_2/h)^{1/2} - 1.389/(1 + h_2/h)\right]\right\} \qquad \text{(A-6)}$$

$$Q = 1.0109 - \tanh^{-1}\left(\left[0.012(w/h) + 0.177(w/h)^2 - 0.027(w/h)^3\right] / (1 + h_2/h)^2\right) \qquad \text{(A-7)}$$

$$\varepsilon_{eff}(f=0) = (\varepsilon_r + 1)/2 + (q)(\varepsilon_r - 1)/2 \qquad \text{(A-8)}$$

ε_r is the dielectric constant of the circuit board dielectric material.

$$q = (q_\infty - q_{ft})q_e \qquad \text{(A-9)}$$

$$q_\infty = [1 + 10(h/w)]^j \qquad \text{(A-10)}$$

$$j = a(w/h)b(\varepsilon_r) \qquad \text{(A-11)}$$

$$a(w/h) = 1+(1/49)\ln\left\{(w/h)^2\left[(w/h)^2 + (1/52)^2\right]/\left[(w/h)^4 + 0.432\right]\right\}$$

$$+ (1/18.7)\ln[1+(w/18.1h)^3] \qquad \text{(A-12)}$$

$$b(\varepsilon_r) = -0.564\left[(\varepsilon_r - 0.9)/(\varepsilon_r + 3.0)\right]^{0.063} \qquad \text{(A-13)}$$

$$q_{ft} = (2/\pi)\ln(2)\left[\frac{t/h}{(w/h)^{1/2}}\right] \qquad \text{(A-14)}$$

$$q_{fe} = \tanh\left[1.043+0.121(h_2/h) - \frac{1.164}{h_2/h}\right] \text{ for } (h_2/h) \geq 1 \qquad \text{(A-15)}$$

The effective dielectric constant ε_{eff} is not really a constant but changes slightly as a function of frequency. The equations provided by Kirschning and Jansen correct the ε_{eff} for frequency. The following equation is used:

$$\varepsilon_{eff}(f) = \varepsilon_r - \frac{\varepsilon_r - \varepsilon_{eff}(f=0)}{1 + P(f)} \qquad \text{(A-16)}$$

where $\varepsilon_{eff}(f)$ is the effective dielectric constant as a function of frequency f, and P(f) is given by the following system of equations:

$$P(f) = P_1P_2[(0.1844 + P_3P_4)10fh]^{1.5763} \qquad \text{(A-17)}$$

$$P_1 = 0.27488 + [0.6315 + 0.525/(1 + 0.15fh)^{20}]u - 0.065683 \exp(-8.7513u) \quad \text{(A-18)}$$

$$P_2 = 0.33622[1 - \exp(-0.03442\varepsilon_r)] \quad \text{(A-19)}$$

$$P_3 = \{0.0363 \exp[-4.6u]\}\{1 - \exp[-(fh/3.87)^{4.97}]\} \quad \text{(A-20)}$$

$$P_4 = 1 + 2.75\{1 - \exp[-(\varepsilon_r/15.916)^8]\} \quad \text{(A-21)}$$

$$u = w/h \quad \text{(A-22)}$$

$$fh \sim h/\lambda_0 \quad \text{(A-23)}$$

λ_0 = wavelength in free space

The wavelength λ in the transmission line at the design frequency is then found from the well known definition of ε_{eff}, given below [38]:

$$\lambda/\lambda_0 = 1/[\varepsilon_{eff}(f)]^{1/2} \quad \text{(A-24)}$$

References

1. Charles M. Howell, *Selection of Multiplier Diodes*, M/A-COM Semiconductor Products Division, Burlington, MA, pp. 4-6.

2. Charles M. Howell, *Selection of Multiplier Diodes*, M/A-COM Semiconductor Products Division, Burlington, MA, p.5, p.24.

3. Charles M. Howell, *Selection of Multiplier Diodes*, M/A-COM Semiconductor Products Division, Burlington, MA, p. 24.

4. ibid.

5. Charles M. Howell, *Selection of Multiplier Diodes*, M/A-COM Semiconductor Products Division, Burlington, MA, pp.32-33.

6. ibid.

7. ibid.

8. Charles M. Howell, *Selection of Multiplier Diodes*, M/A-COM Semiconductor Products Division, Burlington, MA, p.18, p.35.

8. Charles M. Howell, *Selection of Multiplier Diodes*, M/A-COM Semiconductor Products Division, Burlington, MA, p.35.

10. M/A-COM Semiconductor Products Catalog, M/A-COM, Inc., Burlington, MA, 1988, p. 8-20.

11. ibid.

12. Inder Bahl and Prakash Bhartia, *Microwave Solid State Circuit Design*, John Wiley & Sons, New York, 1988, ch. 6.

13. Peter A. Rizzi, *Microwave Engineering Passive Circuits*, Prentice-Hall,Inc., Englewood Cliffs, NJ, 1988, p. 473, (Figure 9-43a).

14. Inder Bahl and Prakash Bhartia, *Microwave Solid State Circuit Design*, John Wiley & Sons, New York, 1988, ch. 6.

15. Inder Bahl and Prakash Bhartia, *Microwave Solid State Circuit Design*, John Wiley & Sons, New York, 1988, pp. 251-254.

16. Inder Bahl and Prakash Bhartia, *Microwave Solid State Circuit Design*, John Wiley & Sons, New York, 1988, pp. 252-53.

17. Inder Bahl and Prakash Bhartia, *Microwave Solid State Circuit Design*, John Wiley & Sons, New York, 1988, p. 257.

18. David M. Pozar, *Microwave Engineering*, Addison-Wesley Publishing Company, Inc., New York, 1990, pp. 494-495.

19. David M. Pozar, *Microwave Engineering*, Addison-Wesley Publishing Company, Inc., New York, 1990, pp. 496-500.

20. Ralph J. Smith, *Circuits, Devices and Systems*, 4th ed., John Wiley & Sons, Inc., New York, 1984, pp. 176-178.

21. Seymour B. Cohn, "Parallel-Coupled Transmission-Line-Resonator Filters," *IRE Trans. Microwave Theory and Techniques*, MTT-6, April 1958, pp. 223-231.

22. Inder Bahl and Prakash Bhartia, *Microwave Solid State Circuit Design*, John Wiley & Sons, New York, 1988, ch. 6.

23. Inder Bahl and Prakash Bhartia, *Microwave Solid State Circuit Design*, John Wiley & Sons, New York, 1988, p. 247, Figure 6.9.

24. Peter A. Rizzi, *Microwave Engineering Passive Circuits*, Prentice-Hall, Inc., Englewood Cliffs, NJ, 1988, p. 473, Figure 9-43.

25. Inder Bahl and Prakash Bhartia, *Microwave Solid State Circuit Design*, John Wiley & Sons, New York, 1988, p. 260, equation (6.16).

26. Peter A. Rizzi, *Microwave Engineering Passive Circuits*, Prentice-Hall,Inc., Englewood Cliffs, NJ, 1988, p. 473, (Figure 9-43b).

27. Inder Bahl and Prakash Bhartia, *Microwave Solid State Circuit Design*, John Wiley & Sons, New York, 1988, p. 260, equation (6.17a).

28. Inder Bahl and Prakash Bhartia, *Microwave Solid State Circuit Design*, John Wiley & Sons, New York, 1988, p. 260, equation (6.17b).

29. Peter A. Rizzi, *Microwave Engineering Passive Circuits*, Prentice-Hall,Inc., Englewood Cliffs, NJ 1988, p. 496, equation (9-132).

30. Inder Bahl and Prakash Bhartia, *Microwave Solid State Circuit Design*, John Wiley & Sons, New York, 1988, p. 263.

31. Peter A. Rizzi, *Microwave Engineering Passive Circuits*, Prentice-Hall, Inc., Englewood Cliffs, NJ, 1988, p. 496, equation (9-133).

32. Peter A. Rizzi, *Microwave Engineering Passive Circuits*, Prentice-Hall, Inc., Englewood Cliffs, NJ, 1988, p. 383, equation (8-32).

33. James Bao-yen Tsui, *Microwave Receivers and Related Components*, Air Force Avionics Lab., Wright-Patterson AFB, Ohio, Library of Congress Catalog no. 83-600566, 1983, pp. 194-201.

34. David M. Pozar, *Microwave Engineering*, Addison-Wesley Publishing Company, Inc., New York, 1990, pp. 288-291.

35. Peter A. Rizzi, *Microwave Engineering Passive Circuits*, Prentice-Hall, Inc., Englewood Cliffs, NJ, 1988, p. 124.

36. James J. Lev, "Synthesize and Analyze Microstrip Lines," *Microwaves and RF*, January 1985, pp. 111-116.

37. M. Kirschning, R. H. Jansen, "Accurate Model for Effective Dielectric Constant of Microstrip with Validity Up to Millimeter-Wave Frequencies," *Electronics Letters*, 1982.

38. Peter A. Rizzi, *Microwave Engineering Passive Circuits*, Prentice-Hall, Inc., Englewood Cliffs, NJ, 1988, p. 198, equation (5-31).

ARMY RESEARCH LABORATORY
ELECTRONICS AND POWER SOURCES DIRECTORATE
CONTRACT OR IN-HOUSE TECHNICAL REPORT
MANDATORY DISTRIBUTION LIST

Defense Technical Information Center*
ATTN: DTIC-OCC
Cameron Station (Bldg 5)
Alexandria, VA 22304-6145
(*Note: Two copies will be sent from STINFO office, Fort Monmouth, NJ)

Director
US Army Material Systems Analysis Actv
ATTN: DRXSY-MP
(1) Aberdeen Proving Ground, MD 21005

Commander, AMC
ATTN: AMCDE-SC
5001 Eisenhower Ave.
(1) Alexandria, VA 22333-0001

Director
Army Research Laboratory
ATTN: AMSRL-D (John W. Lyons)
2800 Powder Mill Road
(1) Adelphi, MD 20783-1145

Director
Army Research Laboratory
ATTN: AMSRL-DD (COL William J. Miller)
2800 Powder Mill Road
(1) Adelphi, MD 20783-1145

Director
Army Research Laboratory
2800 Powder Mill Road
Adelphi, MD 20783-1145
(1) AMSRL-OP-CI-AD (Tech Pubs)
(1) AMSRL-OP-CI-AD (Records Mgt)
(1) AMSRL-OP-CI-AD (Tech Library)

Directorate Executive
Army Research Laboratory
Electronics and Power Sources Directorate
Fort Monmouth, NJ 07703-5601
(1) AMSRL-EP
(1) AMSRL-EP-T (M. Howard)
(1) AMSRL-OP-RM-FM
(22) Originating Office

Advisory Group on Electron Devices
ATTN: Documents
2011 Crystal Drive, Suite 307
(2) Arlington, VA 22202

Commander, CECOM
R&D Technical Library
Fort Monmouth, NJ 07703-5703
(1) AMSEL-IM-BM-I-L-R (Tech Library)
(3) AMSEL-IM-BM-I-L-R (STINFO ofc)

Deputy for Science & Technology
Office, Asst Sec Army (R&D)
(1) Washington, DC 20310

HQDA (DAMA-ARZ-D/
Dr. F.D. Verderame)
(1) Washington, DC 20310

Director
Naval Research Laboratory
ATTN: Code 2627
(1) Washington, DC 20375-5000

Cdr, PM JTFUSION
ATTN: JTF
1500 Planning Research Drive
(1) McLean, VA 22102

Rome Air Development Center
ATTN: Documents Library (TILD)
(1) Griffiss AFB, NY 13441

Dir, ARL Battlefield
Environment Directorate
ATTN: AMSRL-BE
White Sands Missile Range
(1) NM 88002-5501

Dir, ARL Sensors, Signatures,
Signal & Information Processing
Directorate (S3I)
ATTN: AMSRL-SS
2800 Powder Mill Road
(1) Adelphi, MD 20783-1145

Dir, CECOM Night Vision/
Electronic Sensors Directorate
ATTN: AMSEL-RD-NV-D
(1) Fort Belvoir, VA 22060-5677

Dir, CECOM Intelligence and
Electronic Warfare Directorate
ATTN: AMSEL-RD-IEW-D
Vint Hill Farms Station
(1) Warrenton, VA 22186-5100

Cdr, Marine Corps Liaison Office
ATTN: AMSEL-LN-MC
(1) Fort Monmouth, NJ 07703-5033